Electronic Supplementary Material (ESI) for Reaction Chemistry & Engineering.

Making Photochemistry Scalable - An Operationally Simple Falling Film Looping Photoreactor

(Supporting Information)

Shibu Naskar[a,†], Daniel Kowalczyk[c,†], Susital Mal[a], Subrata Das*[a], Debabrata Mandal[b], Prakash Kumar[b], Dirk Ziegenbalg*[c]

[a]National Institute of Technology Patna, Bihar 800005, India,

[b]National Institute of Pharmaceutical Education and Research Hajipur, Bihar 844102, India,

[c]Institute of Chemical Engineering, Ulm University, Albert-Einstein-Allee 11, 89081 Ulm, Germany

[†] These authors contributed equally.

* subratad@nitp.ac.in

* dirk.ziegenbalg@uni-ulm.de

Table of Contents

Materials and Methods

Reagents and Instruments

Reagents and solvents:

All commercially available reagents and solvents were purchased from companies as follows: water: Milli-Q, toluene: SRL, HPLC grade acetonitrile: Merck, N-Bromosuccinimide: TCI, 1,3,5-trimethoxybenzene: TCI, Sodium trifluoromethanesulfinate: TCI, Diacetyl: TCI, Ethyl acetate: SRL, Orthophosphoric acid: SRL, Ammonium acetate buffer: SRL, $CDCl_3$: Cambridge isotope laboratories. Reagents were used directly without purification. All the solvents were purified before use. Inert atmosphere was created with ultra-pure nitrogen gas. Products were purified by column chromatography by using 100-200 mesh silica gel from Merck. Thin layer chromatography (TLC) was performed on Merck silica gel 60 F_{254}.

Instruments:

The reaction mixture was evaporated under reduced pressure on a Buchi rotary evaporator. Peristaltic pumps were bought from Kamoer (KHM-SW3S40). The flow rates of the pumps were increased by increasing the internal diameter of silicon tube from 4 mm to 8 mm.

The yield was determined via HPLC (Agilent 1260 infinity II) equipped with a C18. Column Size: 100 × 3.2 mm, 5 µm. An acetonitrile / 5 mM ammonium acetate buffer (80 mL / 20 mL) was used as mobile phase for the first reaction and acetonitrile/H_2O/H_3PO_4 (40 mL /60 mL /0.1 mL) for the second reaction. A flow rate of 1 mL min^{-1} was applied for the HPLC. The reaction mixture was analyzed using a DAD-UV detector at 230 nm for the first reaction and 266 nm for the second reaction. The HPLC instrument facility was available at NIPER Hajipur.

The isolated products were quantified via NMR spectroscopy using a Bruker 500 MHz FT-NMR spectrometer. The solvent residual peaks of chloroform ($CDCl_3$: δ = 7.26 ppm and δ = 77.0 ppm) were used as references. The NMR instrument facility was availed at SAIF, IIT Patna.

Equipment	Model	Suppliers
1) Rotavapor	Rotavapor R-100	BUCHI
2) Peristaltic pump	KHM-SW3S40	Kamoer
3) 500 MHz NMR spectrometer	ECZ500R/S1	JEOL
4) HPLC	1260 Infinity II	Agilent
5) UV-VIS Spectrophotometer	UV-1780	Shimadzu

Reactor Design

All examined reactor modules were made from borosilicate glass by the central glass blowing facility of IIT Kanpur. Any further details regarding the reactor modules are available upon request. A detailed description of the used photoreactor is given in Figure 1.

Technical drawings of the used 1×A, 2×A and 4×A reactor and irradiation modules with exact dimensions in mm are depicted in Figure 2.

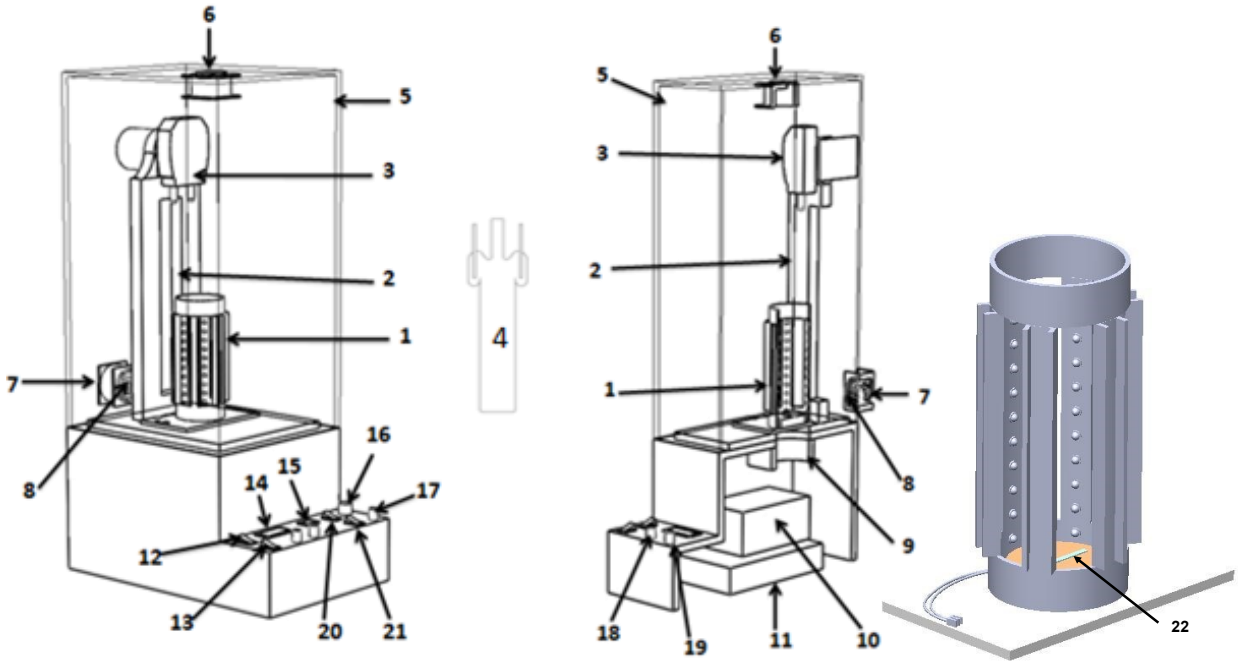

Figure 1: Schematic and cross-sectional view of the falling film looping photoreactor. ***1:*** *irradiation module;* ***2****: adjustable pump holder;* ***3:*** *peristaltic pump;* ***4:*** *reactor module;* ***5:*** *case module;* ***6:*** *cooling fan;* ***7:*** *cooling fan;* ***8:*** *cooling coil;* ***9:*** *magnetic stirrer;* ***10:*** *battery unit;* ***11:*** *12V DC power supply;* ***12:*** *switch for magnetic stirrer;* ***13:*** *switch for irradiation module;* ***14:*** *voltage and current display unit;* ***15:*** *temperature display unit;* ***16:*** *flow rate controller for peristaltic pump;* ***17:*** *cooling fan speed controller;* ***18:*** *current controller;* ***19:*** *magnetic stirrer speed controller;* ***20:*** *switch for pump;* ***21:*** *switch for cooling fan,* ***22:*** *temperature sensor.*

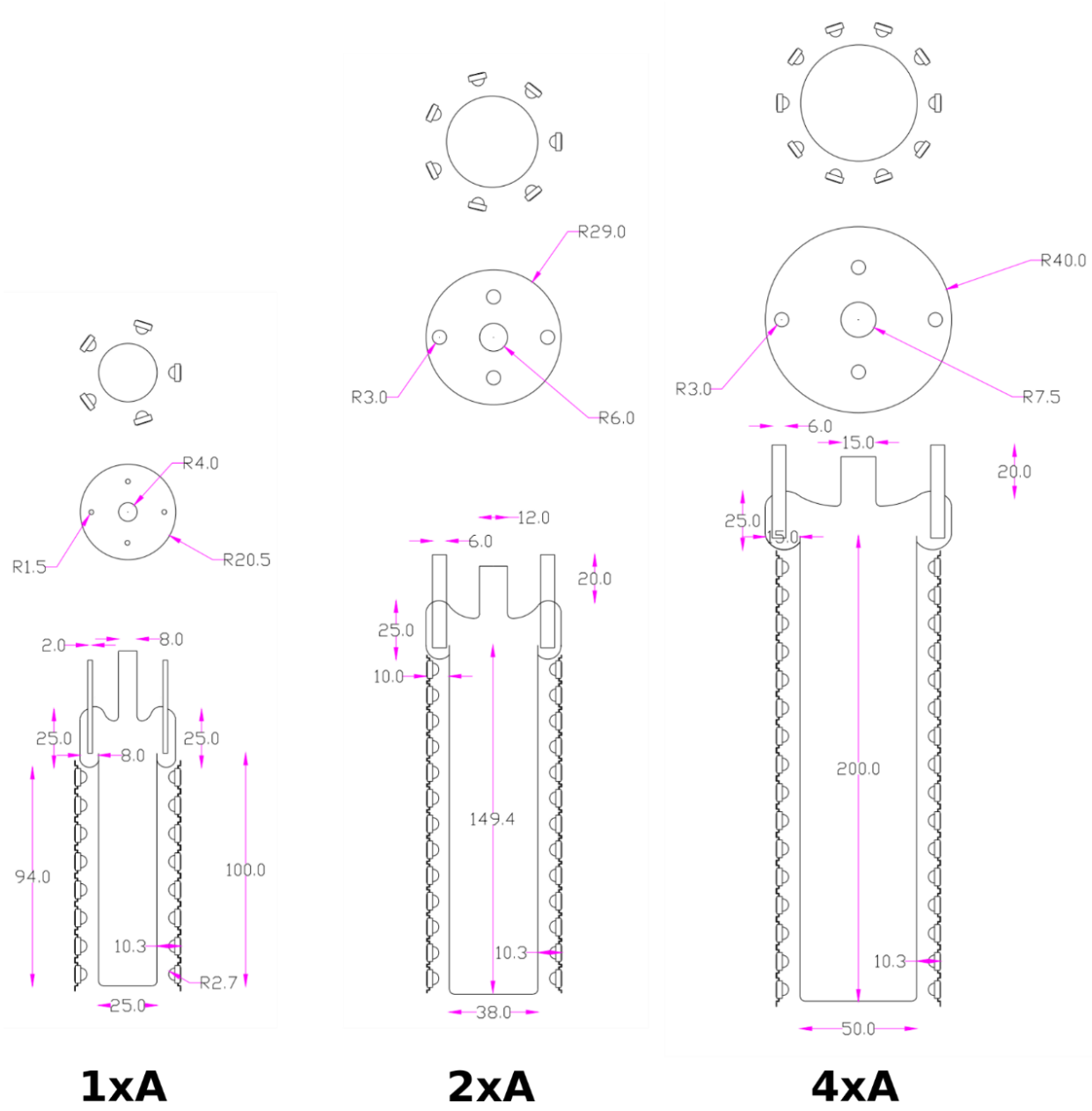

Figure 2: Technical drawing of the 1×A, 2×A and 4×A reactor and irradiation modules with dimensions in mm. The LEDs have a height of 5.3 mm.

Diagrams of the electrical circuits used for the 1A, 2A and 4A irradiation modules can be found in Figure 3

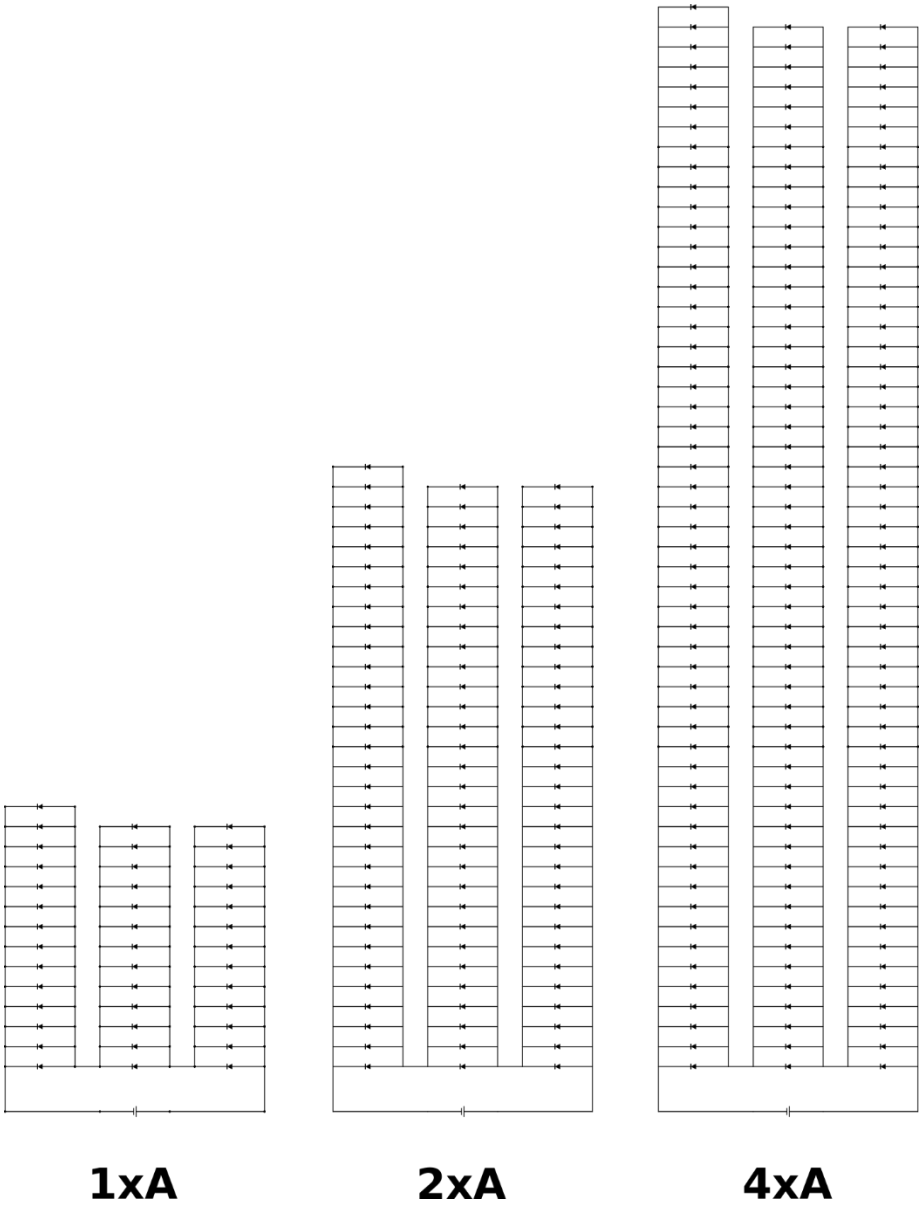

Figure 3: Electrical circuit diagrams of the 1×A, 2×A and 4×A irradiation module.

Detailed Description of the Reactor

The proposed falling film looping photoreactor was designed as a tool for photoreaction optimization and scale-up from a milligram to the gram scale under comparable irradiation and reaction conditions. Therefore, a modular design was implemented to ensure easy adaptation of the reactor components to a changing reaction scale and the needs of experimentalists within photochemical laboratories. The photoreactor can therefore be divided in five main modules:

a) **reactor module,**
b) **irradiation module,**

c) **pump module,**
d) **controller module,**
e) **case module.**

Reactor Module

Three different sized reactor modules made from borosilicate glass, schematically depicted in Figure 2, can be placed inside the corresponding irradiation module. A constant distance of 5 mm between the reactor module and its surrounding LEDs can therefore be realized while mounting the reactor module. The reactor modules are scaled according to their wetted surface (1×A, 2×A and 4×A). The neck portion of the glass corpus of the reactor module is designed to function as distributor for the reaction solution using an integrated spillway. Therefore, the reaction mixture is first pumped up from the center of the reservoir at the bottom of the glass corpus through the outlet hole at the center of the distributor and distributed through four inlet holes to the spillway. The inlet holes are pointed towards the groove at the neck so that the reaction mixture is first collected here and finally overflows the spillway uniformly along the inside surface of the glass container inducing a falling film redirected to the reservoir. During operation the reaction solution is continuously recycled (looped) within the reactor module.

The reactor module can be equipped with a magnetic stirring bar and operated as batch reactor if no falling film is applied.

Irradiation Module

Corresponding to the different sized reactor modules three different irradiation modules, depicted in Figure 2, can be installed in the falling film looping photoreactor. The irradiation module is divides in single LED strips mounted on a heat sinks. The circuit diagrams of the different irradiation modules are depicted in Figure 3. Each LED light strip contains several white LEDs (1×A: 8 LEDs, 2×A: 13 LEDs, 4×A: 16 LEDs). The number of light strips in each irradiation module varies according to the diameter of the reactor module (1×A: 5 LED strips, 2×A: 7 LED strips, 4×A: 10 LED strips). The irradiation modules further can be scaled up or down in the same manner for performing larger or smaller scale chemical reactions. In addition, a rectangular light reflecting mirror which fills the gaps between the light strips can be installed within the irradiation module.

Pump Module

A Kamoer (KHM-SW3S40) peristaltic pump was used for all the experiments (see component 3, Figure 1). The internal silicon tube of the pump was replaced to increase the maximum flow rate of the pump realized by increasing the internal diameter form 4 mm to 8 mm . This increased the flow rate of the pump from about 600 mL · min^{-1} to about 1100 mL · min^{-1}. Silicon tubes of 2 mm, 4 mm and 6 mm internal diameter were used (for 1×A, 2×A and 4×A reactor module, respectively) for the recirculation of the reaction mixture. The motor speed of the pump and thus the flow rate is controlled by a controlling module. The used peristaltic pump allows the application of inert atmosphere to the performed reactions. The dark volumes of the internal tubing of the used pump and the external tubing used for the

recirculation of the reaction mixture in dependence of the used reactor module and reaction scale are listed in

Table 1. The adjustable pump stand (see component 2, Figure 1) is used to adjust the mounting position of the pump to the used reactor module.

Figure 4: Falling film looping photoreactor setup equipped with different irradiation modules 1×A module (left), 2×A module (middle) and back view of the case module (right).

Table 1: Total dark volumes of used pumps (internal tubing) and external tubing for the used reactor modules and scales.

reactor module	reaction volume / mL	quantity pumps	diameter internal tubing / mm	dark volume pump / mL	diameter external tubing / mm	dark volume external tubing / mL
1×A	10-30	1	8	2.4	2	0.7
2×A	50	1	8	2.4	4	1.2
4×A	100	2	8	4.8	6	3.6

Controller Module

The control unit was designed to be simple, and allow easy operation of the falling film looping photoreactor in the laboratory. A magnetic stirrer (see component 9, Figure 1) can be utilized if the reactor is operated as batch reactor without the application of a falling film. A battery unit (see component 10, Figure 1) was included to the controller module allowing reactor operation to continue even during power failures. For the main operation of the reactor a 12 V, 10 A DC power supply (see component 11, Figure 1) was used. Current controlling systems (see component 18, Figure 1) along with a display unit for the applied voltage and current (see component 14, Figure 1) allow control over the optical power of the irradiation modules. Moreover, the flow rate controller (see component 16, Figure 1) maintains a specific

flow rate during a reaction. There is also an inbuilt heating equipment, for reactions needed external heating.

Case Module

A light shield was used to safeguard the eyes of the user from high-energy visible light. To overcome the challenges of the heat removal process, two cooling fans (see component 6 and 7, Figure 1) and a cooling coil (see component 8, Figure 1) as introduced. The cooling coil can be connected to a cryostat enabling operating temperatures of 25-60^{0}C with controllable fan speed.

Photoreactions

Reaction 1: Benzylic Bromination of Toluene using N-Bromosuccinimide

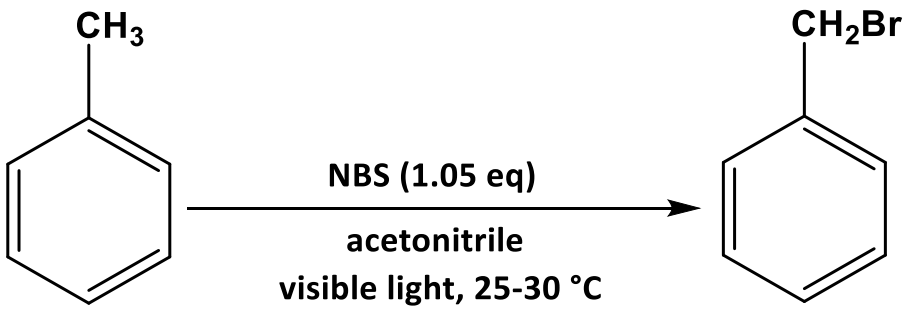

Figure 5: Reaction scheme of the benzylic bromination of toluene in acetonitrile using N-bromosuccinimide.

Dynamic Viscosity of Toluene Acetonitrile Mixtures

The dynamic viscosity of toluene acetonitrile mixtures at 298.15 K in dependence of the molar fraction of toluene is depicted in Figure 6.[1] The dynamic viscosity of the toluene acetonitrile mixture used for reaction 1 was calculated based on the molar fraction of toluene (0.027) using the linear regression

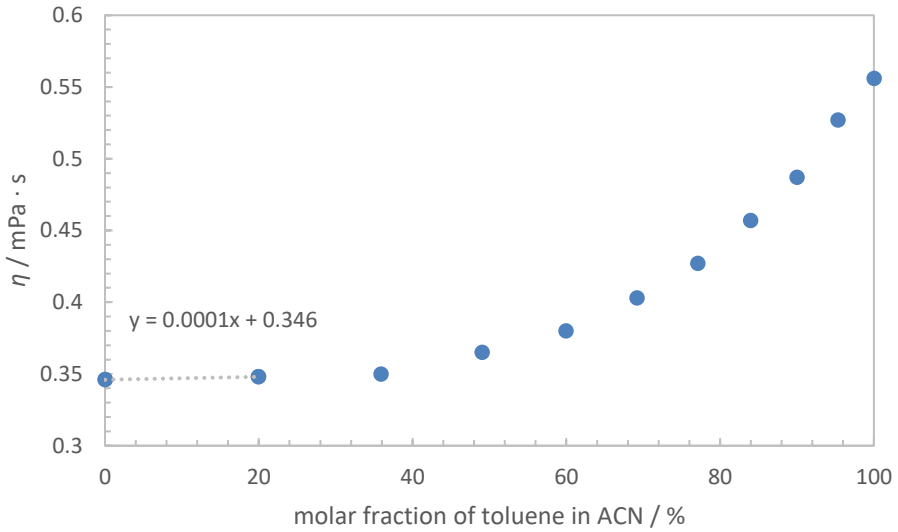

Figure 6: Dynamic viscosity of toluene/acetonitrile mixtures at 298.15 K in dependence of the molar fraction of toluene.

depicted in Figure 6. The calculated dynamic viscosity of the binary reaction mixture used for the reaction 1 is η = 0.34627 mPa · s.

HPLC Calibration with Product Standard and Reaction Analysis

The yield of the bromination product was determined by HPLC using a calibration curve. Therefore, five different concentrations of the product standard benzyl bromide were used. The HPLC diagrams and the resulting calibration function are depicted in Figure 7. The corresponding area values of the HPLC analysis are listed in Table 2.

All measurements of the bromination product were performed in an Agilent 1260 infinity-II equipped with a C18 column with a size of 100 × 3.2 mm, 5µm. An acetonitrile/5 mM ammonium acetate buffer in the volume ratio of 80:20 was used as mobile phase with a flow rate of 1 mL ·min^{-1}. A DAD-UV at a wavelength of 230 nm was used a detector.

Table 2: HPLC data related to different Standard concentrations of benzyl bromide.

benzyl bromide concentration / µg · mL^{-1}	$peak\ area$ / mAU · s
0.18	13
1.80	46
4.50	131
9.00	253
45.00	1296

For the quantification of the brominated product, samples were taken in 2-min intervals from the reactor. For HPLC analysis the samples were diluted using a factor 200 for the photon flux optimization experiment and 130 for the all-other experiments. The yield was determined using the calibration function depicted in Figure 7.

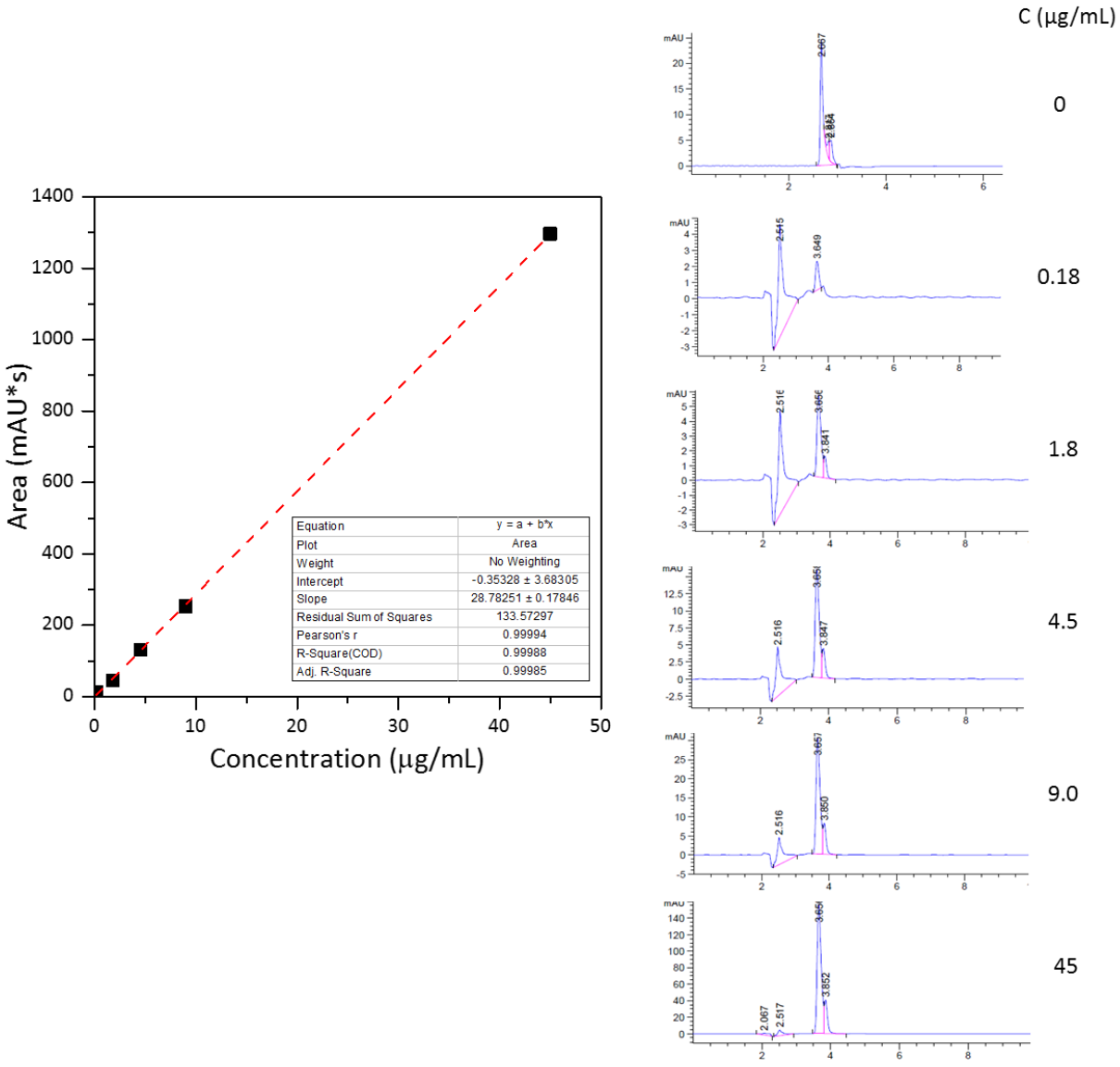

Figure 7: Calibration curve of five different known benzyl bromide concentrations and corresponding HPLC chromatograms at five different concentrations.

Effect of the Light Reflecting Mirror

The design of the irradiation module includes rectangular light reflecting mirrors which fill the gaps between the light strips to allow internal reflection. The influence of the mirror application on the bromination is depicted in Figure 8. For all other experiments no mirror was used.

Conditions: current = 2 A, total radiant power = 8.56 W, irradiance = 109 mW · cm^{-2}, total photon flux = 38 µmol · s^{-1}, space velocity = 15 min^{-1}, reaction volume = 10 mL, module: 1×A

Table 3: Kinetics of benzylic bromination using NBS with and without mirror.

t / min	$peak\ area\ mirror$ / mAU · s	Y_{mirror} / %	$peak\ area\ no\ mirror$ / mAU · s	$Y_{no\ mirror}$ / %
0	0	0	0	0
2	4197.85	22	767.77	6
4	11735.3	62	4839.75	39
6	16223.5	86	9931.13	81
8	17419.1	92	10536.7	85

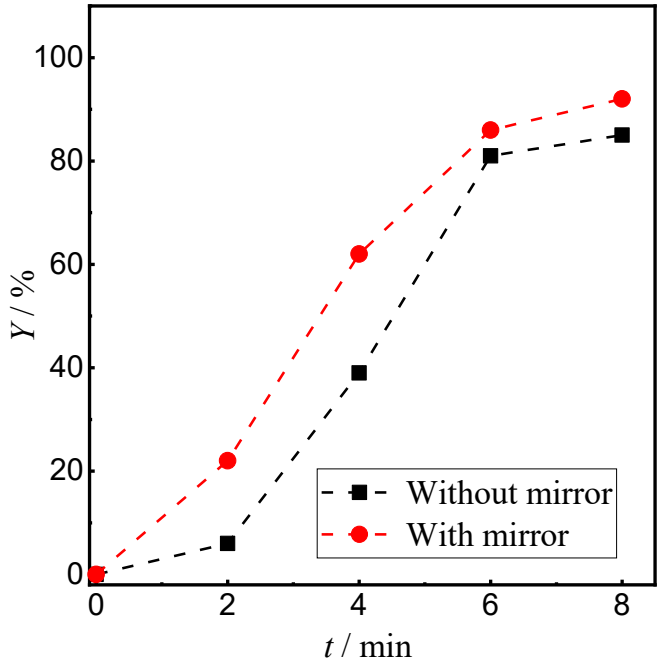

Figure 8: Time studies for benzylic bromination with and without light reflecting mirror.

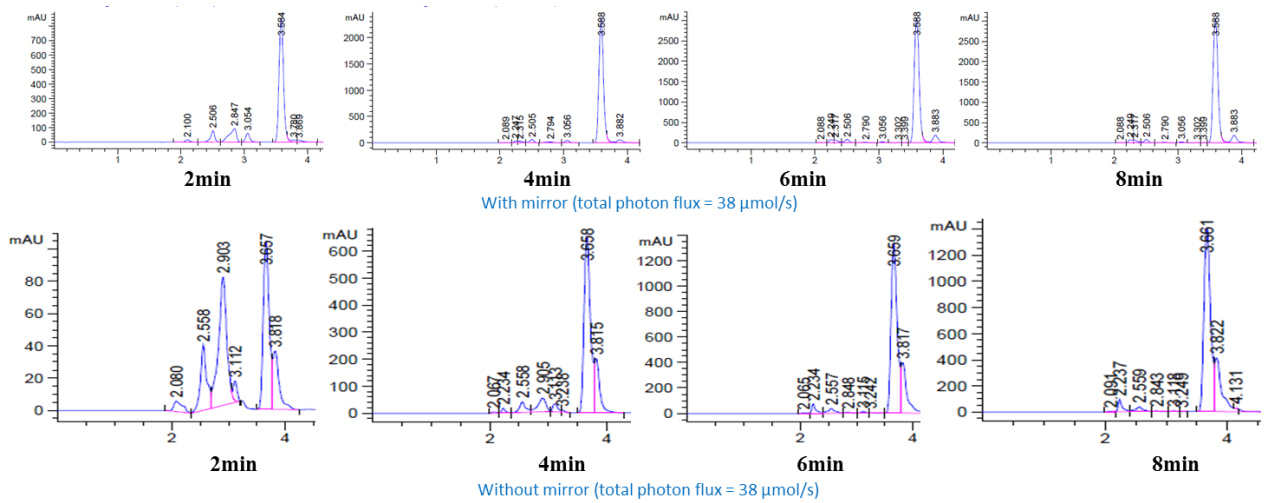

Figure 9: HPLC chromatograms obtained from the time studies of benzylic bromination reaction with and without mirror.

Photon flux Optimization

HPLC chromatograms and the corresponding peak areas of the investigations on the influence of the photon flux on the reaction performance are depicted in Figure 10 and listed in Table 4, Table 5 and Table 6.

Conditions: reactor module = 1×A, current = 1 A, total radiant power = 4.71 W, irradiance = 60.1 mW · cm^{-2}, total photon flux = 21 µmol · s^{-1}, space velocity = 15 min^{-1}. reaction volume = 10 mL.

Table 4: Kinetics of benzylic bromination using NBS with photonic flux 21 µmoL · s^{-1}.

t / min	$peak\ area$ / mAU · s	Y / %
0	0	0
2	299.95	2
4	1764.76	14
6	4938.56	40
8	10789	87
10	11550.5	94

Conditions: reactor module = 1×A, current = 2 A, total radiant power = 8.56 W, irradiance = 109 mW · cm^{-2}, total photon flux = 38 µmol · s^{-1}, space velocity = 15 min^{-1}, reaction volume = 10 mL.

Table 5: Kinetics of benzylic bromination using NBS with photonic flux 38 µmoL · s^{-1}.

t / min	$peak\ area$ / mAU · s	Y / %
0	0	0
2	767.77	6
4	4839.75	39
6	9931.13	81
8	10536.7	85
10	11637.3	94

Conditions: reactor module = 1×A, current = 2.5A, total radiant power = 10.32 W, irradiance = 131.4 mW · cm^{-2}, total photon flux = 46 µmol · s^{-1}, space velocity = 15 min^{-1} , reaction volume = 10 mL

Table 6: Kinetics of benzylic bromination using NBS with photonic flux 46 µmoL · s^{-1}.

t / min	$peak\ area$ / mAU · s	Y / %
0	0	0
2	2532.82	21
4	10448.5	85
6	11317.3	92
8	10734.2	87
10	10478.5	85

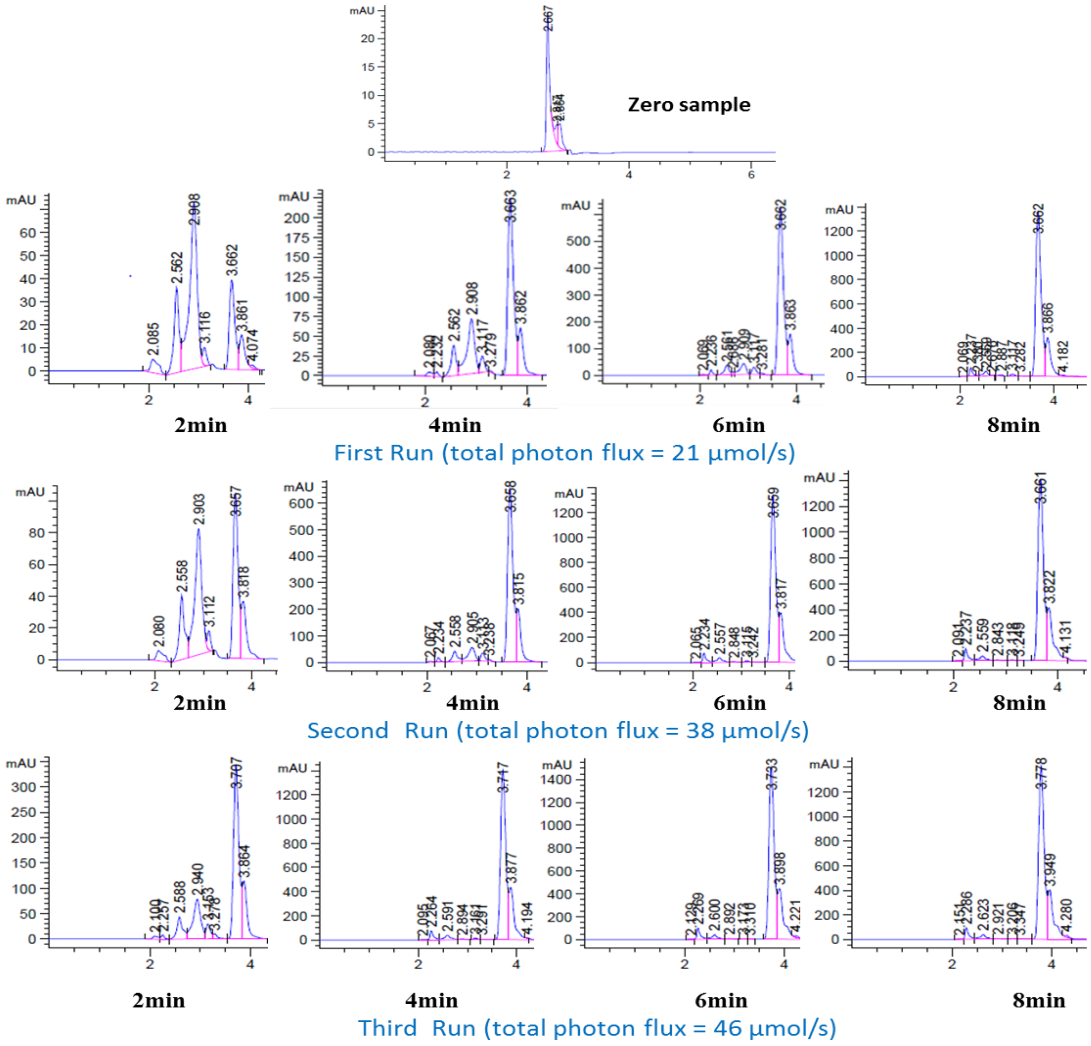

Figure 10: HPLC chromatograms obtained from the time studies of benzylic bromination reaction at three different photonic flux with 1×A module.

Optimization of the Reaction Volume

HPLC chromatograms and the corresponding peak areas of the investigations on the influence of the reaction volume on the reaction performance can are depicted in Figure 12 and listed in Table 7, Table 8 and Table 9. Figure 11 shows the filled reactors.

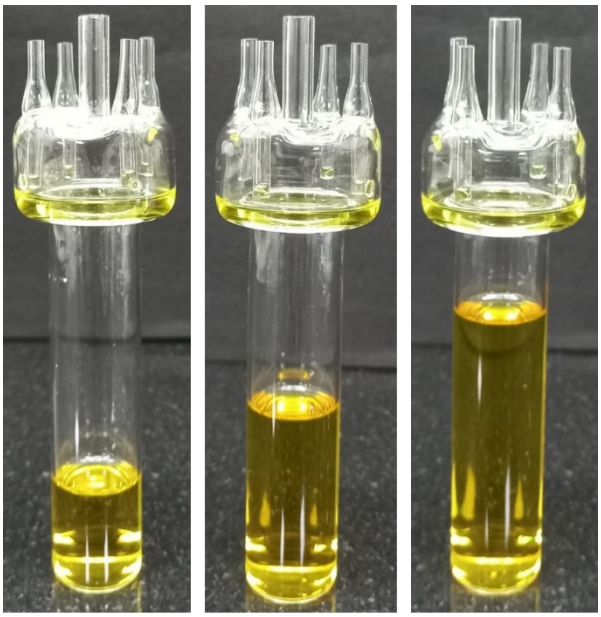

*Figure 11: 1xA reactor module filled with **a** 10 mL, **b** 20 mL and **c** 30 mL of reaction solution corresponding to a surface to volume ratio of 785 $m^2 \cdot m^{-3}$, 393 $m^2 \cdot m^{-3}$ and 262 $m^2 \cdot m^{-3}$.*

First Run (1×A reactor module)

Conditions: reactor module = 1×A, current = 2.5 A , total radiant power = 10.32 W, irradiance = 131.4 mW $\cdot cm^{-2}$, total photon flux = 46 µmol $\cdot s^{-1}$, space velocity = 15 min^{-1} , reaction volume = 10 mL , surface to volume ratio = 785 $m^2 \cdot m^{-3}$

Table 7: Kinetics of benzylic bromination using NBS with photonic flux 46 µmoL s^{-1} and 10 mL reaction volume.

t / min	$peak\ area$ / mAU · s	Y / %
0	0	0
2	2532.82	21
4	10448.5	85
6	11317.3	92
8	10734.2	87
10	10478.5	85
12	10467.0	85

Second Run (1×A reactor module)

Conditions: reactor module = 1×A, current = 2.5 A, total radiant power = 10.32 W, irradiance = 131.4 mW · cm^{-2}, total photon flux = 46 µmol · s^{-1}, space velocity = 15 min^{-1}, reaction volume = 20 mL , surface to volume ratio = 393 $m^2 \cdot m^{-3}$

Table 8: Kinetics of benzylic bromination using NBS with photonic flux 46 µmoL s^{-1} and 20 mL reaction volume.

t / min	$peak\ area$ / mAU · s	Y / %
0	0	0
2	6802.5	36
4	17114.8	90
6	17996.4	95
8	18672.5	98
10	17723.8	94
12	17845.5	94

Third Run (1×A reactor module)

Conditions: reactor module = 1×A, current = 2.5 A, total radiant power = 10.32 W, irradiance = 131.4 mW · cm^{-2}, total photon flux = 46 µmol · s^{-1}, space velocity = 15 min^{-1}, reaction volume = 30 mL , surface to volume ratio = 262 $m^2 \cdot m^{-3}$

Table 9: Kinetics of benzylic bromination using NBS with photonic flux 46 µmoL s^{-1} and 30 mL reaction volume.

t / min	$peak\ area$ / mAU · s	Y / %
0	0	0
2	1000.717	5
4	3659.96	19
6	9575.23	51
8	12494.7	66
10	16172.9	85
12	15124.9	80

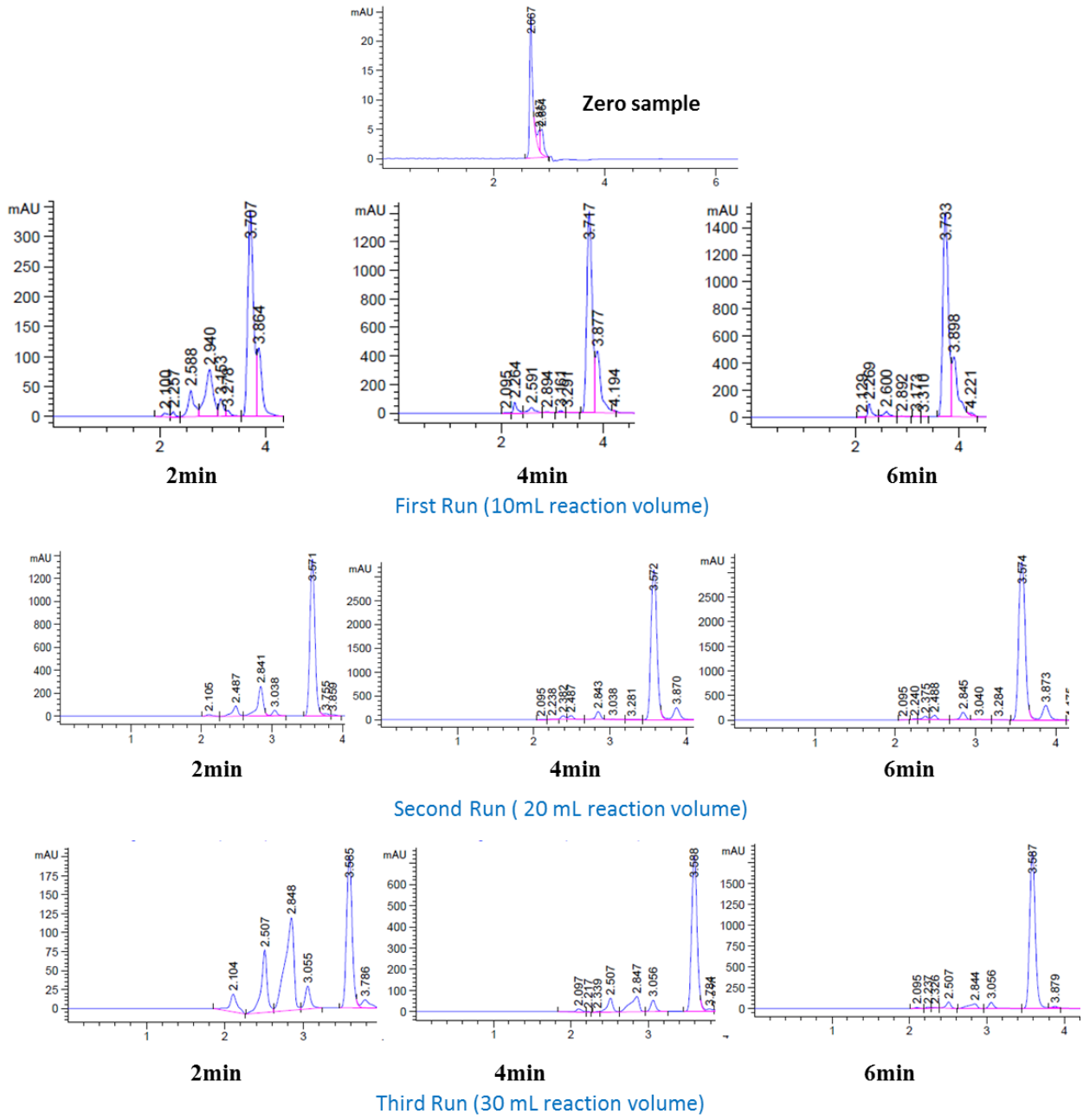

Figure 12: HPLC chromatograms obtained from the time studies of benzylic bromination at 10 mL, 20 mL and 30 mL reaction volume with corresponding surface area of 785 $m^2 m^{-3}$, 393 $m^2 m^{-3}$ and 262 $m^2 m^{-3}$, respectively, by using the 1×A reactor module.

Comparison Between the Application of a Falling Film Versus no Falling Film

HPLC chromatograms and the corresponding peak areas of the investigations on the influence of the falling film in comparison to no falling film on the reaction performance are depicted in Figure 13 and listed in Table 10 and Table 11.

First Run (20 mL reaction mixture with the surface flow, 1×A reactor module)

Conditions: current = 2.5 A, total radiant power = 10.32 W, irradiance = 131.4 mW · cm^{-2}, total photon flux = 46 µmol · s^{-1}, space velocity = 15 min^{-1}, reaction volume = 20 mL.

Table 10: Kinetics of benzylic bromination using NBS with photonic flux of 46 µmoL s^{-1} and falling film.

t / min	$peak\ area$ / mAU · s	Y / %
0	0	0
2	6802.5	36
4	17114.8	90
6	17996.4	95
8	18672.5	98
10	17723.8	94
12	17845.5	94

Second Run (20 mL reaction mixture without flow, 1×A reactor module)

Conditions: current = 2.5 A , total radiant power = 10.32 W, irradiance = 131.4 mW · cm^{-2}, total photon flux = 46 µmol · s^{-1}, space velocity = 0 min^{-1} , reaction volume = 20 mL.

Table 11: Kinetics of benzylic bromination using NBS with photonic flux of 46 µmoL s^{-1} and without falling film.

t / min	$peak\ area$ / mAU · s	Y / %
0	0	0
2	1063.30	6
4	8282.55	44
6	13206.8	70
8	16919.3	89
10	17802.5	94
12	17685.6	94

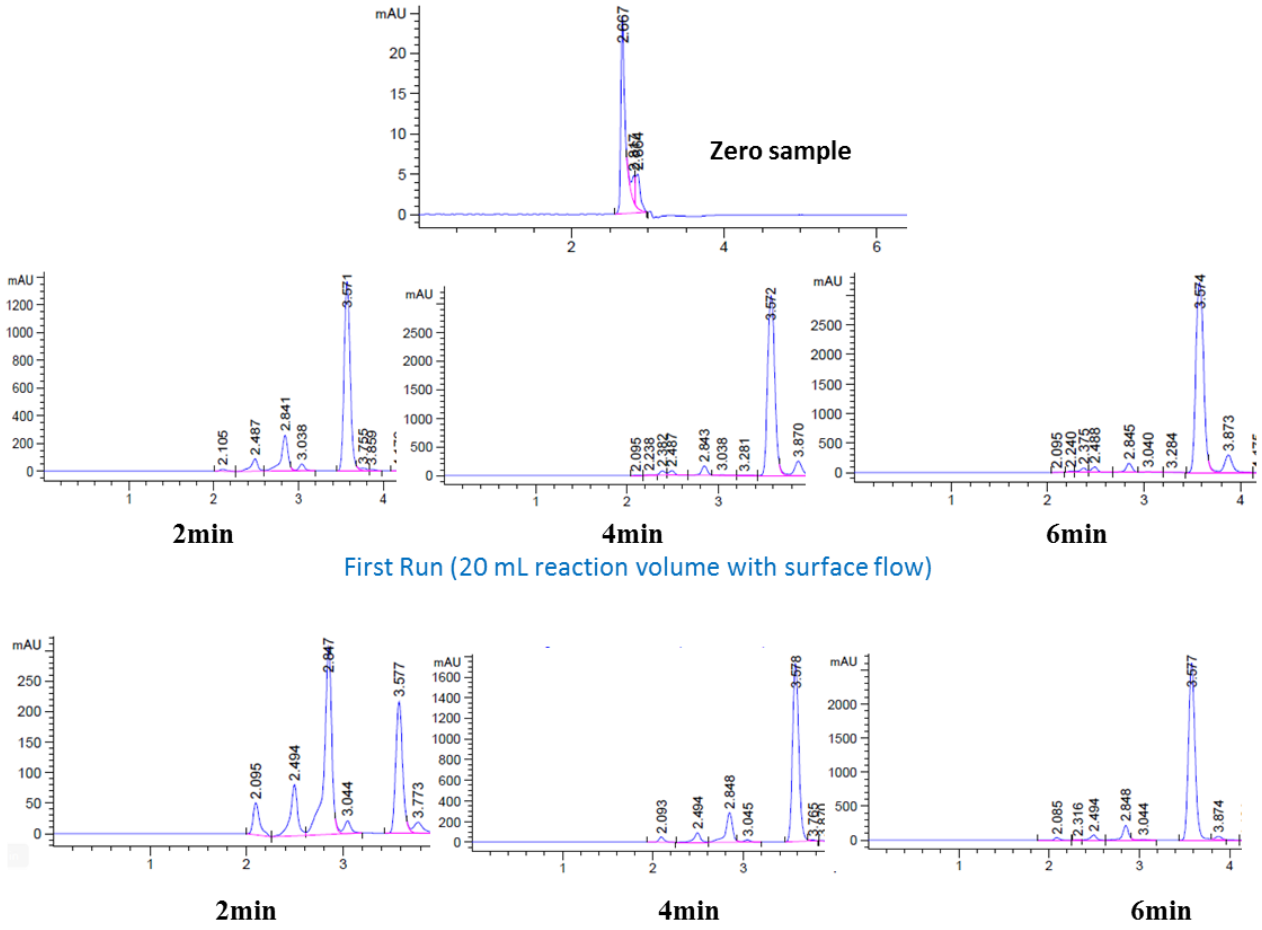

Figure 13: HPLC chromatograms obtained from the time studies of benzylic bromination reaction with and without flow by using 1×A module.

Space Velocity Variations

HPLC chromatograms and the corresponding peak areas of the investigations on the influence space velocity on the reaction performance are depicted in Figure 14 and listed in Table 12 Table 13 and Table 14.

First Run

Conditions: current = 5 A, total radiant power = 22.81 W, irradiance = 127.4 mW · cm^{-2}, total photon flux = 102 µmol · s^{-1}, space velocity = 1.5 min^{-1}, reaction volume = 50 mL.

Table 12: Kinetics of benzylic bromination using NBS and with a space velocity of 1.5 min^{-1}.

t / min	$peak\ area$ / mAU · s	Y / %
0	0	0
2	734.70	4
4	732.58	4
6	738.09	4
8	831.28	4
10	783.02	4
12	1000.43	5

Second Run

Conditions: current = 5 A, total radiant power = 22.81 W, irradiance = 127.4 mW · cm^{-2}, total photon flux = 102 µmol · s^{-1}, space velocity = 5 min^{-1}, reaction volume = 50 mL.

Table 13: Kinetics of benzylic bromination using NBS and with a space velocity of 5 min^{-1}.

t / min	$peak\ area$ / mAU · s	Y / %
0	0	0
2	1603.40	8
4	5739.20	30
6	11486	61
8	15160.2	80
10	15783.7	83
12	17006.5	90

Third Run

Conditions: current = 5 A, total radiant power = 22.81 W, irradiance = 127.4 mW · cm^{-2}, total photon flux = 102 µmol · s^{-1}, space velocity = 10 min^{-1}, reaction volume = 50 mL

Table 14: Kinetics of benzylic bromination using NBS and with a space velocity of 10 min^{-1}.

t / min	$peak\ area$ / mAU · s	Y / %
0	0	0
2	2918.31	15
4	13936.1	74
6	16912.3	83
8	16560.5	89
10	17661.4	93
12	17640.2	93

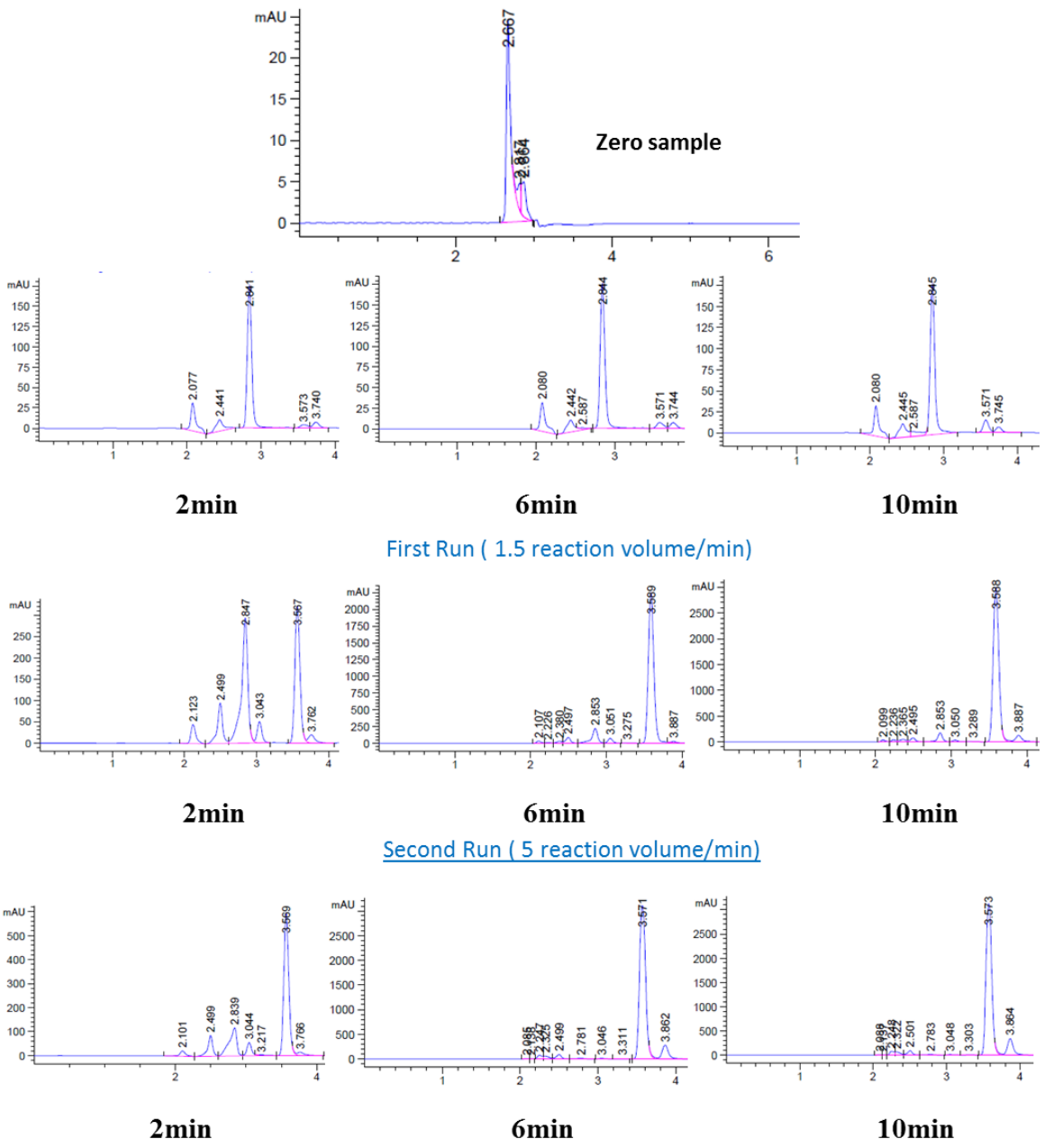

Figure 14: HPLC chromatograms obtained from the time studies of benzylic bromination reaction with different space velocity by using 2×A reactor module.

Scale Up

HPLC chromatograms and the corresponding peak areas of the investigations on the influence of the reaction scale on the reaction performance are depicted in Figure 15 and Figure 16 and listed in Table 15, Table 16, Table 17 and Table 18.

460 mg scale (1×A reactor module)

Conditions: current = 2.5 A, total radiant power = 10.32 W, irradiance = 131.4 mW · cm^{-2}, total photon flux = 46 µmol · s^{-1}, space velocity = 15 min^{-1}, reaction volume = 10 mL

Table 15: Kinetics of benzylic bromination using NBS with 460 mg scale.

t / min	$peak\ area$ / mAU · s	Y / %
0	0	0
2	2532.82	21
4	10448.5	85
6	11317.3	92
8	10734.2	87
10	10478.5	85

920 mg scale (1×A reactor module)

Conditions: current = 2.5 A, total radiant power = 10.32 W, Irradiance = 131.4 mW · cm^{-2}, total photon flux = 46 µmol · s^{-1}, space velocity = 15 min^{-1}, reaction volume = 20 mL

Table 16: Kinetics of benzylic bromination using NBS with 920 mg scale.

t / min	$peak\ area$ / mAU · s	Y / %
0	0	0
2	6802.5	36
4	17114.8	90
6	17996.4	95
8	18672.5	98
10	17723.8	94
12	17845.5	94

2300 mg scale (2×A reactor module)

Conditions: current = 5 A, total radiant power = 22.81 W, irradiance = 127.4 mW · cm^{-2}, total photon flux = 102 µmol · s^{-1}, space velocity = 10 min^{-1}, reaction volume = 50 mL

Table 17: Kinetics of benzylic bromination using NBS with 2300 mg scale.

t / min	$peak\ area$ / mAU · s	Y / %
0	0	0
2	2918.31	15
4	13936.1	74
6	16912.3	83
8	16560.5	89
10	17661.4	93
12	17640.2	93

4600 mg scale (4×A reactor module)

Conditions: current = 10 A, total radiant power = 41.27 W, irradiance = 131.4 mW · cm^{-2}, total photon flux = 185 µmol · s^{-1}, space velocity = 15 min^{-1}, reaction volume = 100

Table 18: Kinetics of benzylic bromination using NBS with 4600 mg scale.

t / min	$peak\ area$ / mAU · s	Y / %
0	0	0
2	1949.95	10
4	10293.6	54
6	16370	86
8	17622.9	93
10	17571.9	93
12	18105.15	96

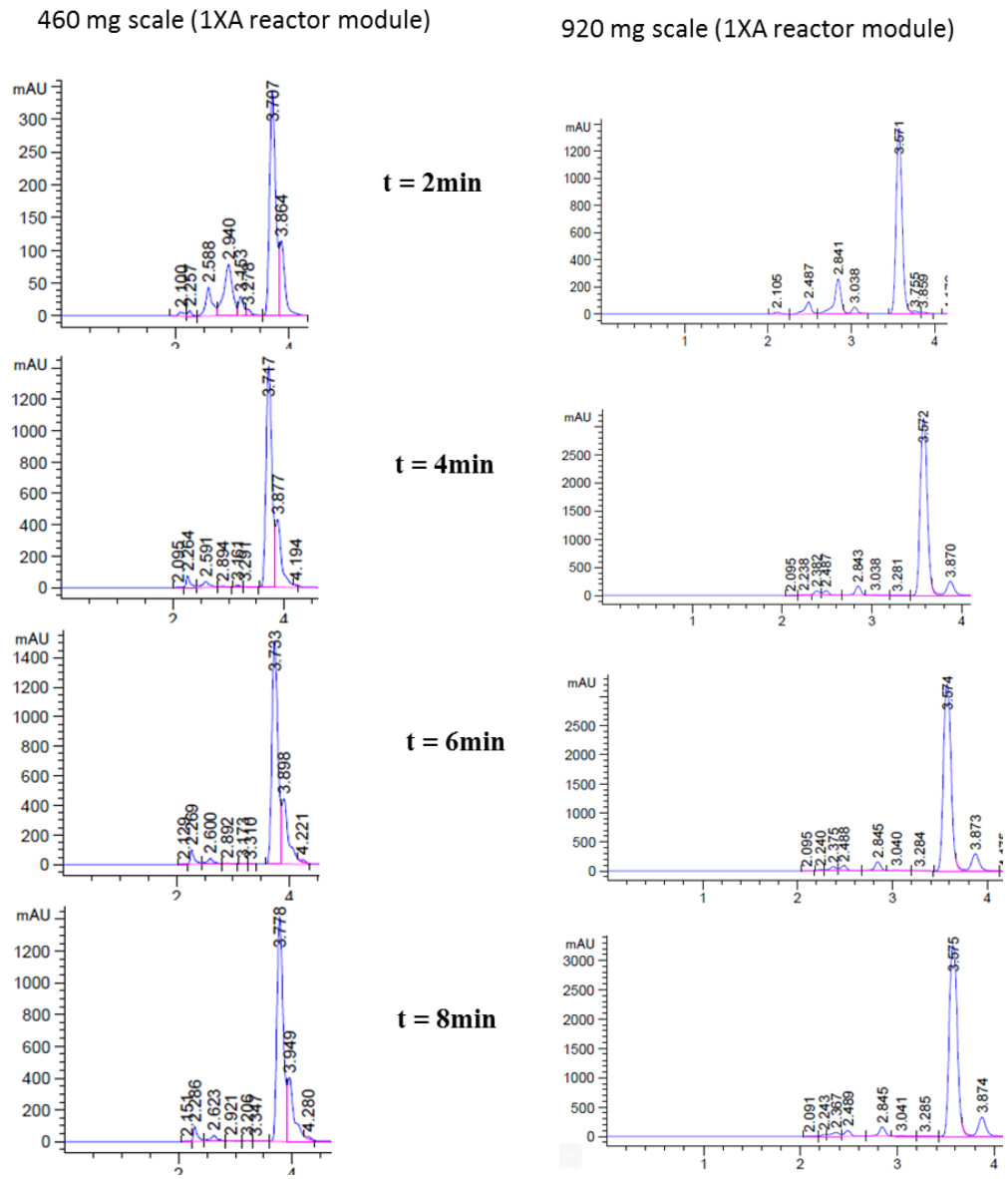

Figure 15: HPLC chromatograms obtained from the time studies of benzylic bromination reaction with 460 mg and 920 mg scale by using 1×A reactor module.

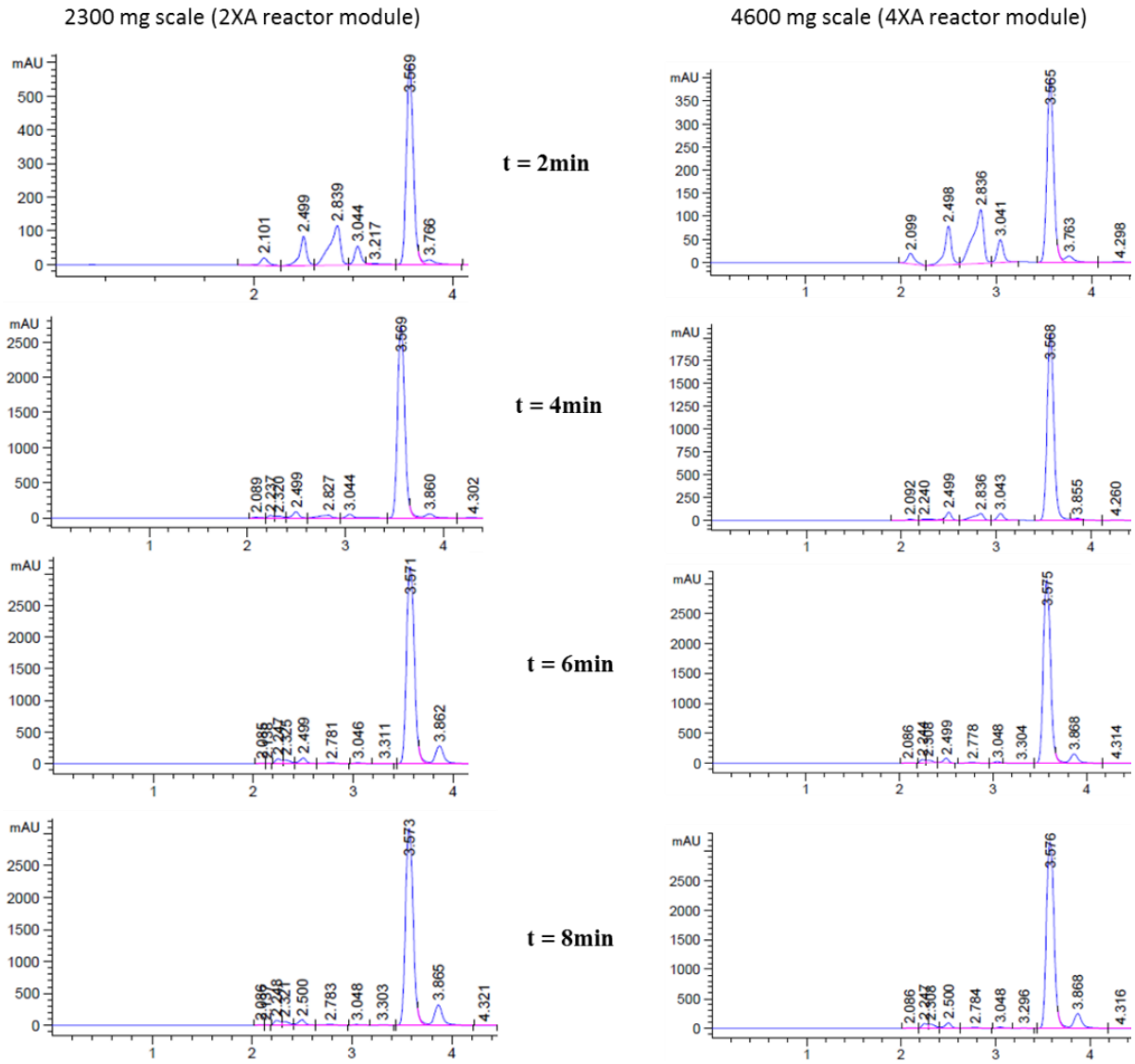

Figure 16: HPLC chromatograms obtained from the time studies of benzylic bromination reaction with 2300 mg and 4600 mg scale by using 2×A and 4×A reactor module respectively.

Product Purification and NMR Analysis

Procedure: The isolated yield of benzyl bromide was determined from the 4.6 g scale (100 mL) reaction. A mixture of toluene (49.92 mmol, 4599.63 mg) and NBS (52.42 mmol, 9329.71 mg) was placed in the reactor, and 100 ml of acetonitrile solvent was added to it. After the completion of the reaction, 100 mL reaction mixture were collected from the reactor and the solvent was evaporated under reduced pressure. The residue was shaken with 1:1 petroleum ether and diethyl ether. The precipitate was discarded and the solvent was evaporated again. This process was repeated until there was no precipitate. 7829 mg liquid benzyl bromide were obtained which is ~92%. The product was synthesized and separated according to the reported procedure and the spectroscopic data is in agreement with the literature. [2]

^{1}H NMR (300 MHz, CDCl3): δ 7.31−7.18 (m, 5H), 4.39 (s, 2H).

^{13}C NMR (75 MHz, CDCl3): δ 137.8, 129.1, 128.8, 128.4, 33.6.

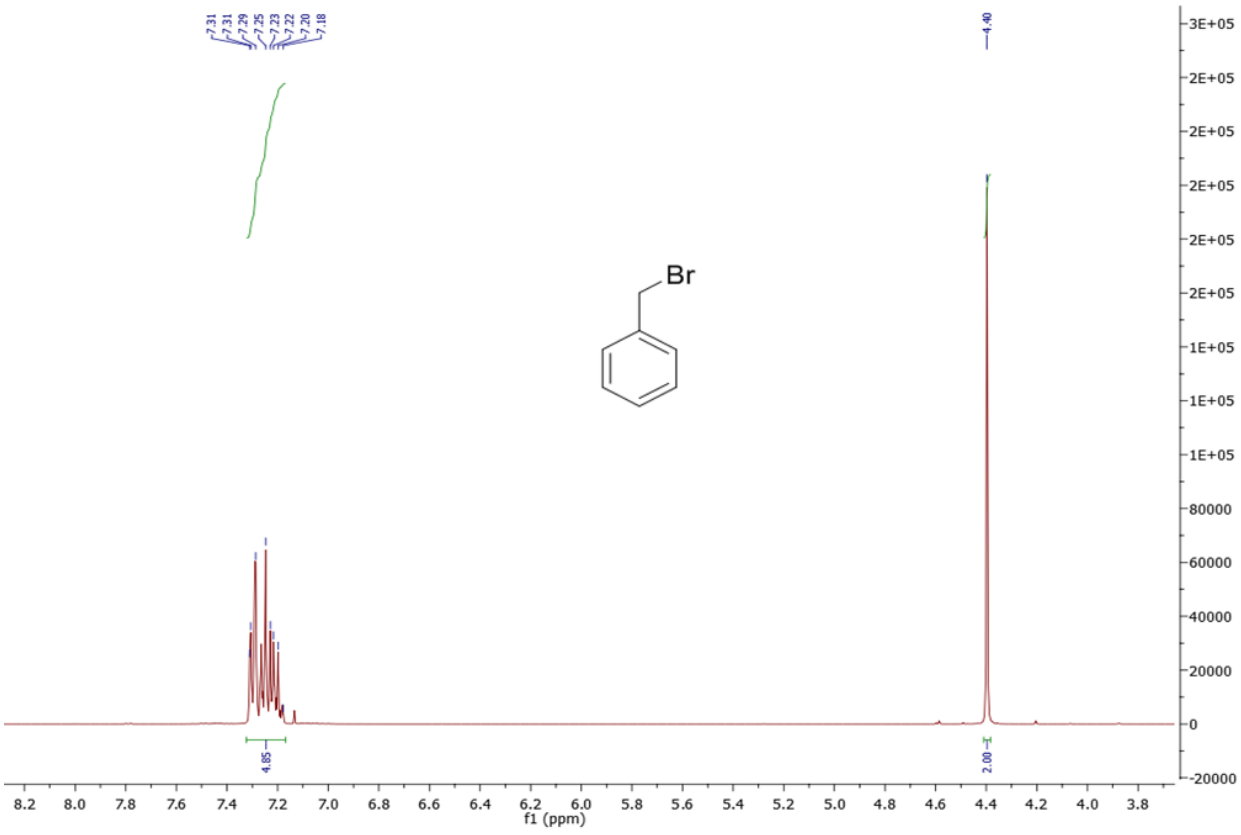

Figure 17: ^{1}H NMR spectra of benzyl bromide.

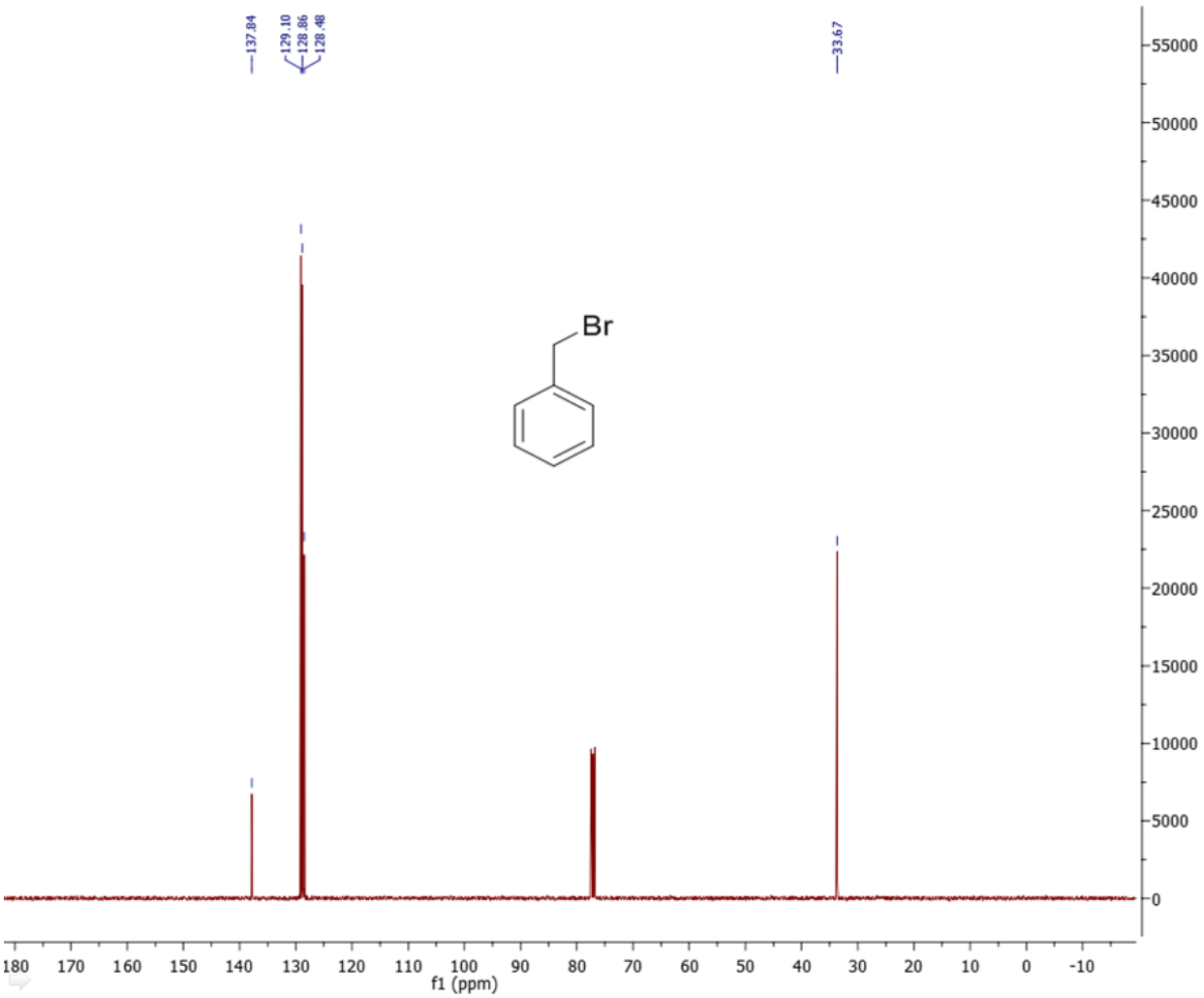

Figure 18: ^{13}C NMR spectra of benzyl bromide.

Reaction 2: Trifluoromethylation with Langlois Reagent

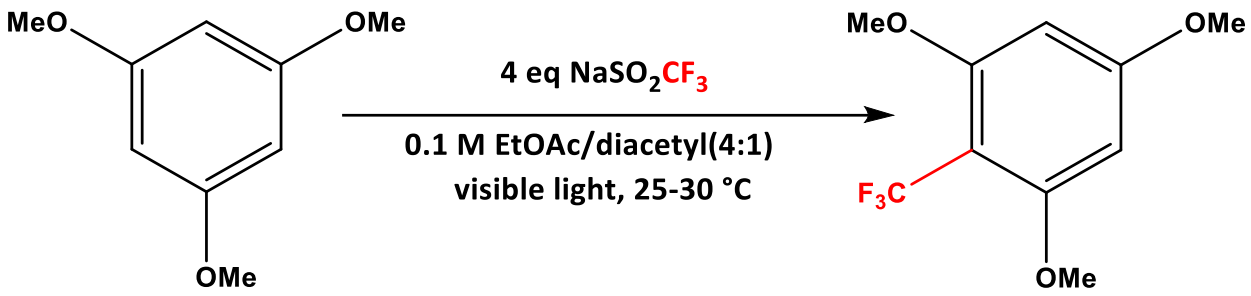

Figure 19: Reaction scheme of trifluoromethylation of 1,3,5-trimethoxybenzene with Langlois reagent.

HPLC Calibration with Reactant Standard and Reaction Analysis

The conversion of 1,3,5-trimethoxybenzene was determined by HPLC using a calibration curve. Therefore, four different concentrations of the educt standard 1,3,5-trimethoxybenzene were used. The HPLC diagrams and the resulting calibration function are depicted in Figure 20. The corresponding area values of the HPLC analysis are listed in Table 19.

All measurements of the bromination product were performed in an Agilent 1260 infinity-II equipped with a C18 column with a size of 100 × 3.2 mm, 5µm. A mobile phase consisting of acetonitrile / H_2O / H_3PO_4 (40 mL / 60 mL / 0.1 mL) was used with a flow rate of 1 mL · min^{-1}. A DAD-UV at a wavelength of 266 nm was used a detector.

Table 19: HPLC data related to different standard concentrations of 1, 3, 5-trimethoxybenzene.

1, 3, 5-Trimethoxybenzene concentration / µg ·mL^{-1}	$\boldsymbol{peak\ area}$ **/ mAU · s**
0	0
10	40
20	56
25	77
30	94

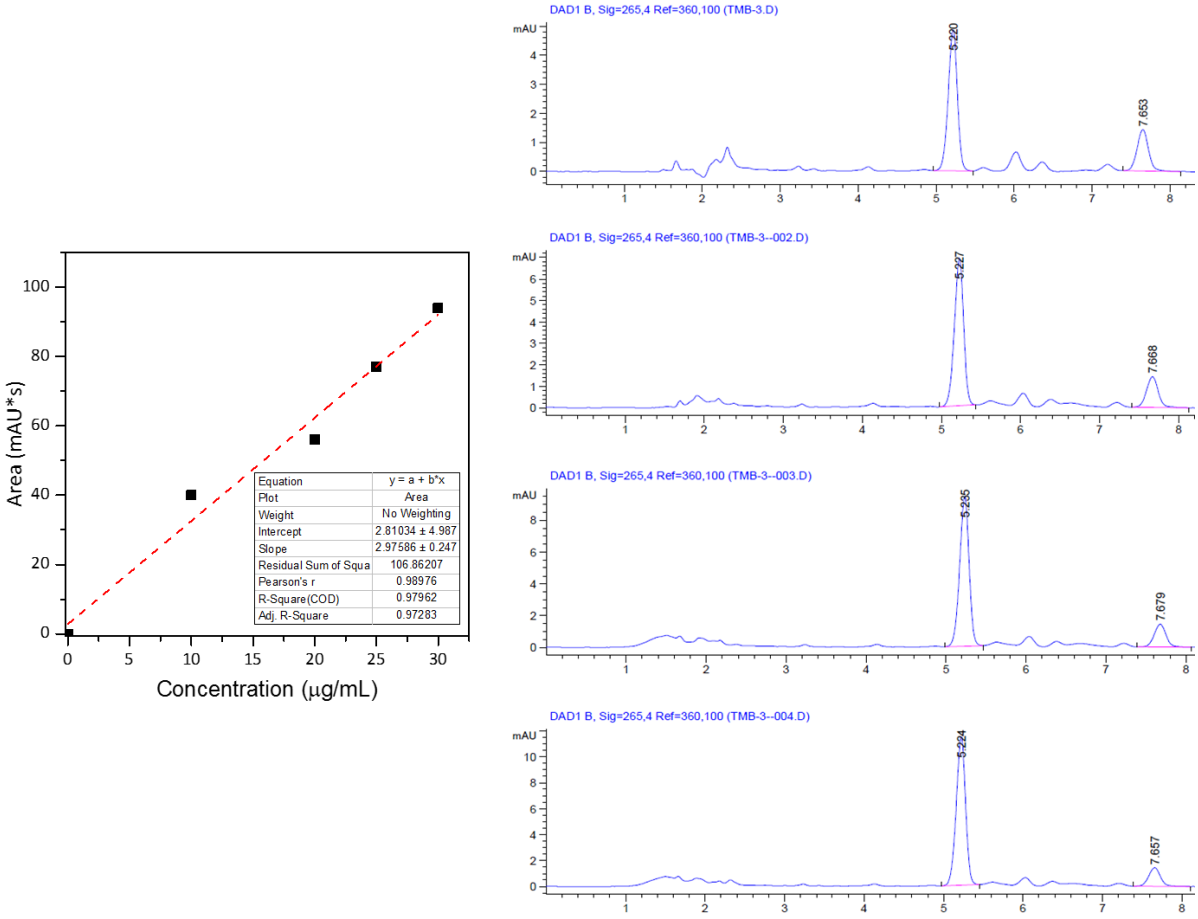

Figure 20: Calibration curve of four different 1, 3, 5-trimethoxybenzene concentration and corresponding HPLC chromatograms.

For every reaction of 1,3,5-trimethoxybenzene, sodium trifluoromethylsulfinate (4 eq) were dissolved in 0.1 M ethyl acetate/diacetyl (4:1) mixture. Nitrogen gas was sparged at 0 °C for 15 minutes. The glassware was made air-tight and put into the irradiation module. Voltage, electrical current and space velocity were set as needed. For HPLC analysis 5 µL of the reaction mixture was taken at 10 min, 20 min, 25 min and 30 min from the reactor and diluted 200 times. The conversion was determined using the calibration function depicted in Figure 20.

Scale Up

HPLC chromatograms and the calculated corresponding peak areas for the influence of the reaction scale on the reaction performance are depicted in Figure 21 and Figure 22 and listed in Table 20, Table 21, Table 22 and

Table 23. As per the obtained result, no side products could be observed. The reaction was stopped at the desired time, so over-irradiation was avoided. Generally, side products of a photochemical reaction are observed if the reaction rate is very slow or the reaction is carried out continuously after sufficient product formation. MacMillan[44] used a 26-watt CFL and an integrated photoreactor for the trifluoromethylation reaction. Their study revealed that the side product started forming after one hour with the integrated photoreactor, and for CFLs, it started forming after 10 hours. For the experiments reported here, the reaction finished within 20 minutes. So over-irradiation may not have happened.

168 mg scale (1×A reactor module)

Conditions: current = 2.5 A, total radiant power = 10.32 W, irradiance = 131.4 mW · cm^{-2}, total photon flux = 46 µmol · s^{-1}, space velocity = 15 min^{-1}, reaction volume = 10 mL

Table 20: Kinetics of trifluoromethylation of 1, 3, 5-Trimethoxybenzene with 168 mg scale.

t / min	$peak\ area$ / mAU · s	X / %
0	0	0
5	125.05	51
10	121.10	53
15	75.30	71
20	23.67	92
25	12.89	96

336 mg scale (1×A reactor module)

Conditions: current = 2.5 A, total radiant power = 10.32 W, irradiance = 131.4 mW · cm^{-2}, total photon flux = 46 µmol · s^{-1}, space velocity = 15 min^{-1}, reaction volume = 20 mL

Table 21: Kinetics of trifluoromethylation of 1, 3, 5-Trimethoxybenzene with 336 mg scale..

t / min	$peak\ area$ / mAU · s	X / %
0	0	0
5	137.95	46
10	133.40	48
15	88.51	66
20	24.41	91
25	16.55	94

840 mg scale (2×A reactor module)

Conditions: current = 5 A, total radiant power = 22.81 W, Irradiance = 127.4 mW · cm^{-2}, total photon flux = 102 µmol · s^{-1}, space velocity = 15 min^{-1}, reaction volume = 50 mL

Table 22: Kinetics of trifluoromethylation of 1, 3, 5-Trimethoxybenzene with 840 mg scale.

t / min	$peak\ area$ / mAU · s	X / %
0	0	0
5	127.26	50
10	137.08	46
15	89.02	65
20	31.20	89
25	15.28	95

1.68 g scale (4×A reactor module)

Conditions: current = 10 A, total radiant power = 41.27 W, irradiance = 131.4 mW · cm^{-2}, total photon flux = 185 µmol · s^{-1}, space velocity = 15 min^{-1}, reaction volume = 100 mL

Table 23: Kinetics of trifluoromethylation of 1, 3, 5-Trimethoxybenzene with 1.68 g scale.

t / min	$peak\ area$ / mAU · s	X / %
0	0	0
5	135.95	47
10	140.63	45
15	88.06	66
20	26.96	90
25	15.78	95

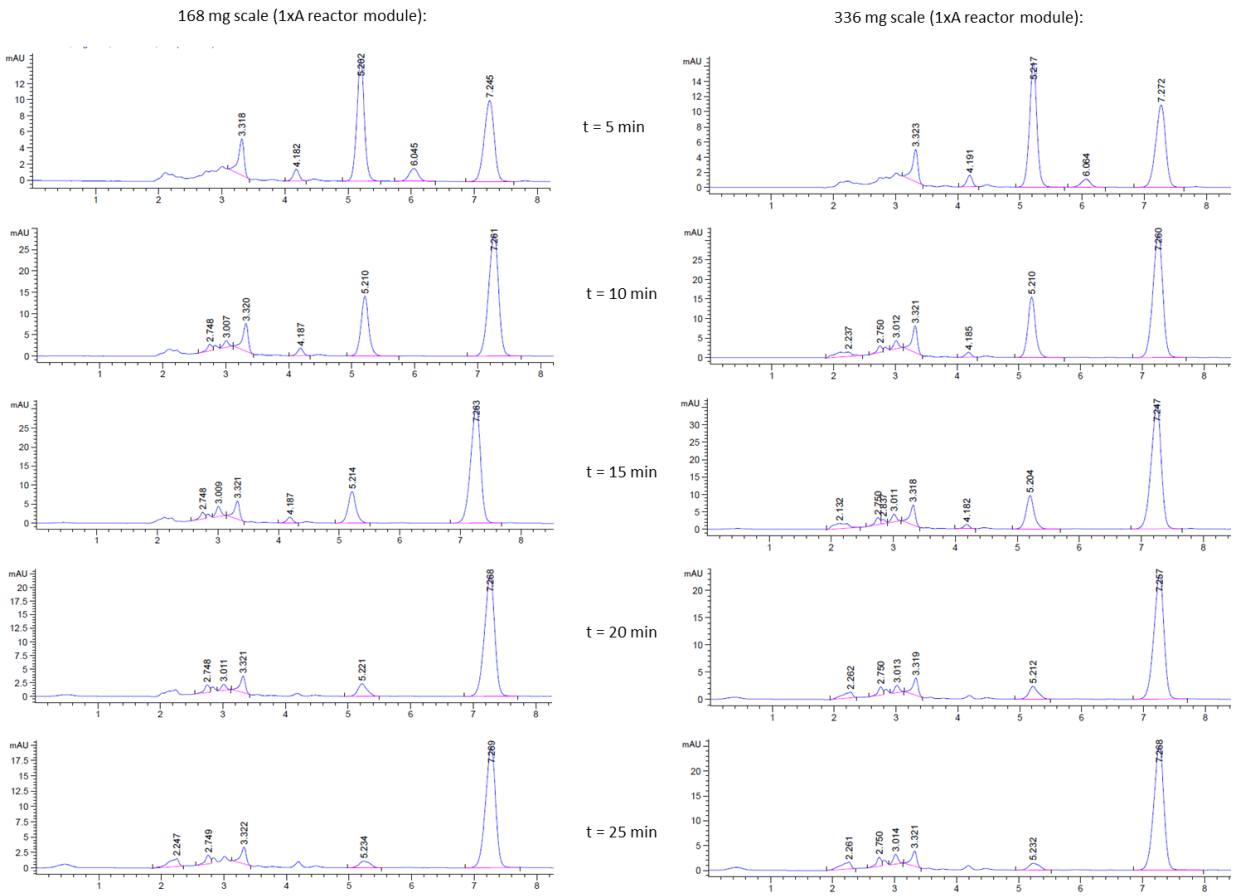

Figure 21: HPLC chromatograms obtained from the time studies for the trifluoromethylation of 1, 3, 5-trimethoxybenzene with 168 mg and 336 mg scale respectively with 1×A reactor module.

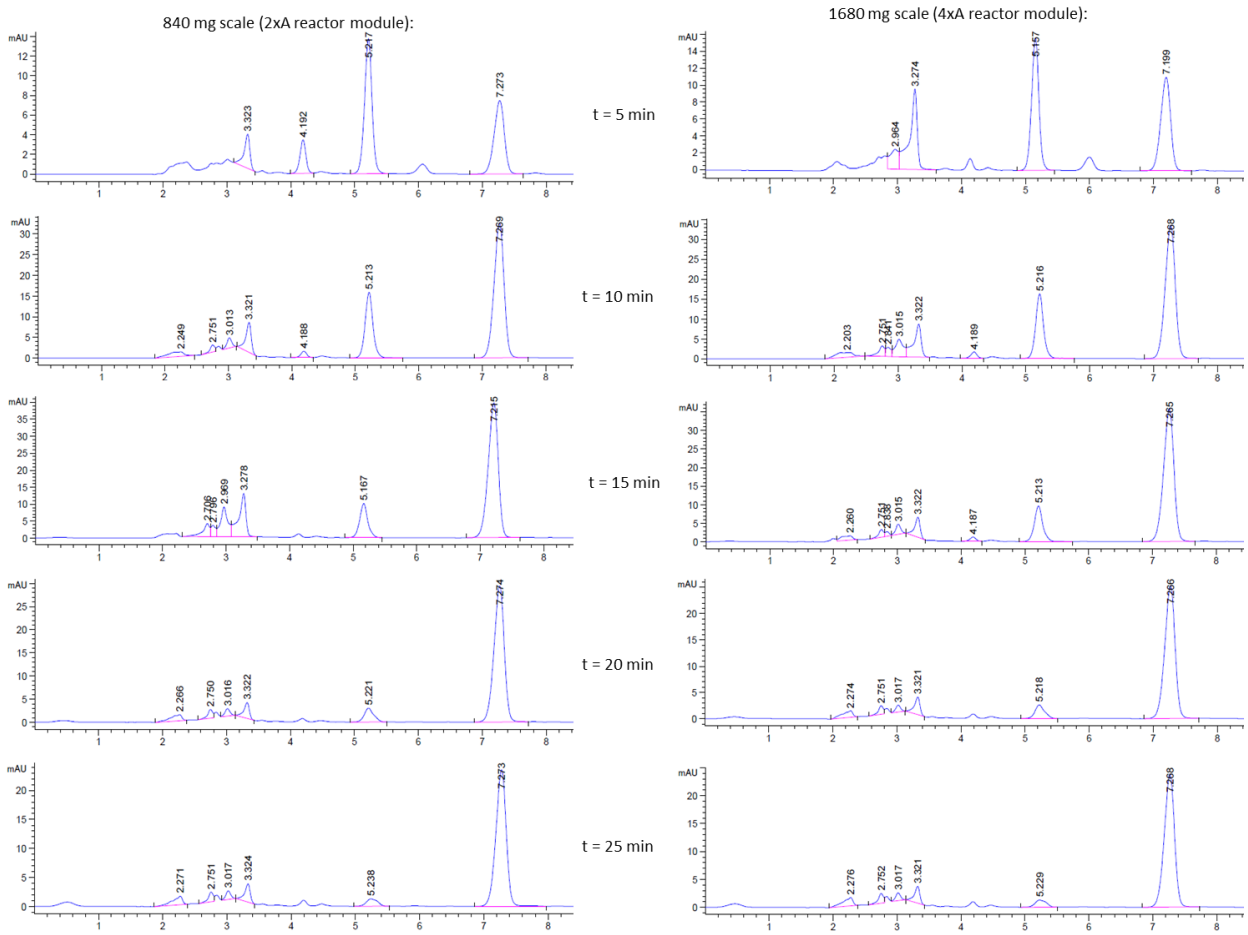

Figure 22: HPLC chromatograms obtained from the time studies for the trifluoromethylation of 1, 3, 5-trimethoxybenzene with 840 mg and 1680 mg scale with 2×A and 4×A reactor module respectively.

Product Purification and NMR Analysis

Procedure: The isolated yield of the trifluoromethyl derivative of 1,3,5-trimethoxybenzene was determined from the 1.681 g scale (100 mL). A mixture of 1,3,5-trimethoxybenzene (9.99 mmol, 1681 mg) and sodium trifluoromethylsulfinate (39.96 mmol, 6236.15 mg) was placed in a 4:1 ethyl acetate/diacetyl solvent ratio. Then, nitrogen gas was sparged at 0 °C for 15 minutes. The glassware was made airtight and put into the irradiation module. After the completion of the reaction, 100 mL reaction mixture collected from the reactor was filtered by using Whatman filter paper. The white color residue was washed using ethyl acetate and then hexane. Then the solvent was evaporated, and the crude product was purified by column chromatography. 2063 mg (~87%) product was separated. The product was synthesized and separated according to the reported procedure and the spectroscopic data is in agreement with the literature. [3]

^{1}H NMR (500 MHz, $CDCl_3$): δ 6.13 (s, 2H), 3.84 (s, 9H).

^{13}C NMR (126 MHz, $CDCl_3$) δ 163.5, 160.4, 124.3 (q, $J_{C\text{-}F}$ = 276.8 Hz, CF3), 100.4 (q, $J_{C\text{-}F}$ = 30.2 Hz), 91.3, 56.2, 55.4

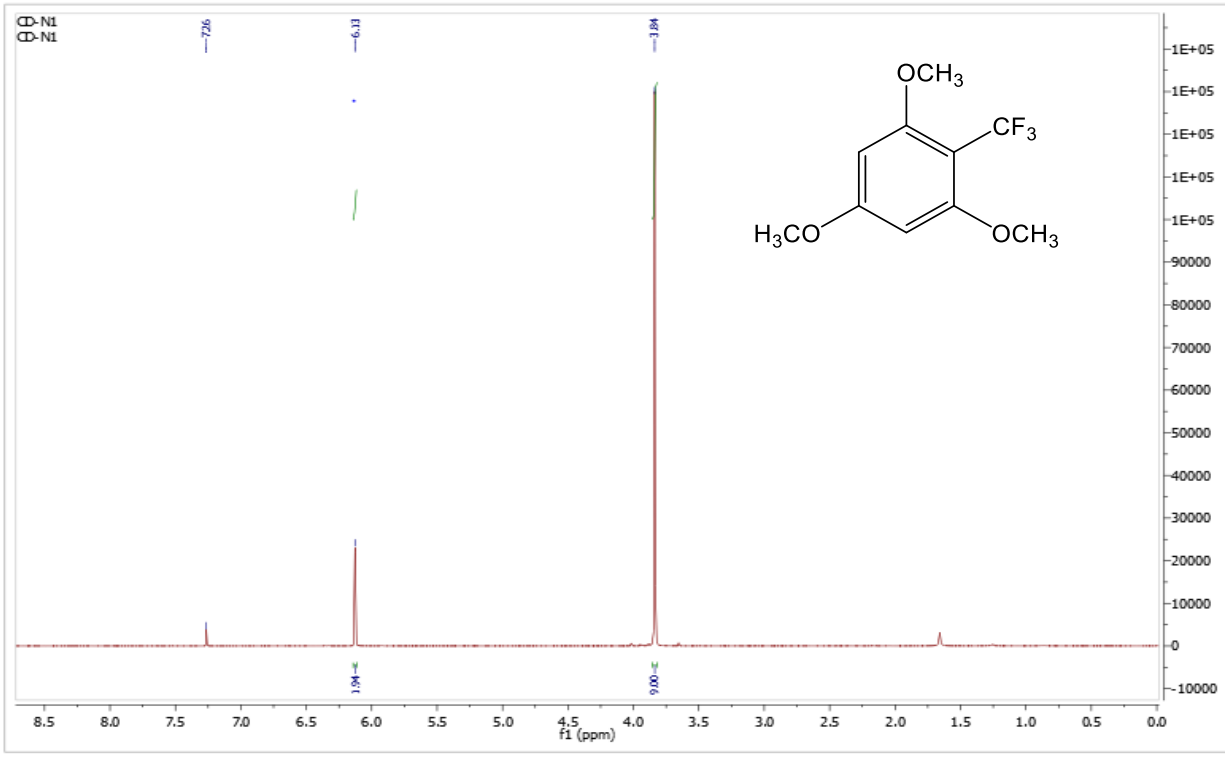

Figure 24: ^{1}H NMR spectra of 1,3,5-trimethoxy-2-(trifluoromethyl)benzene.

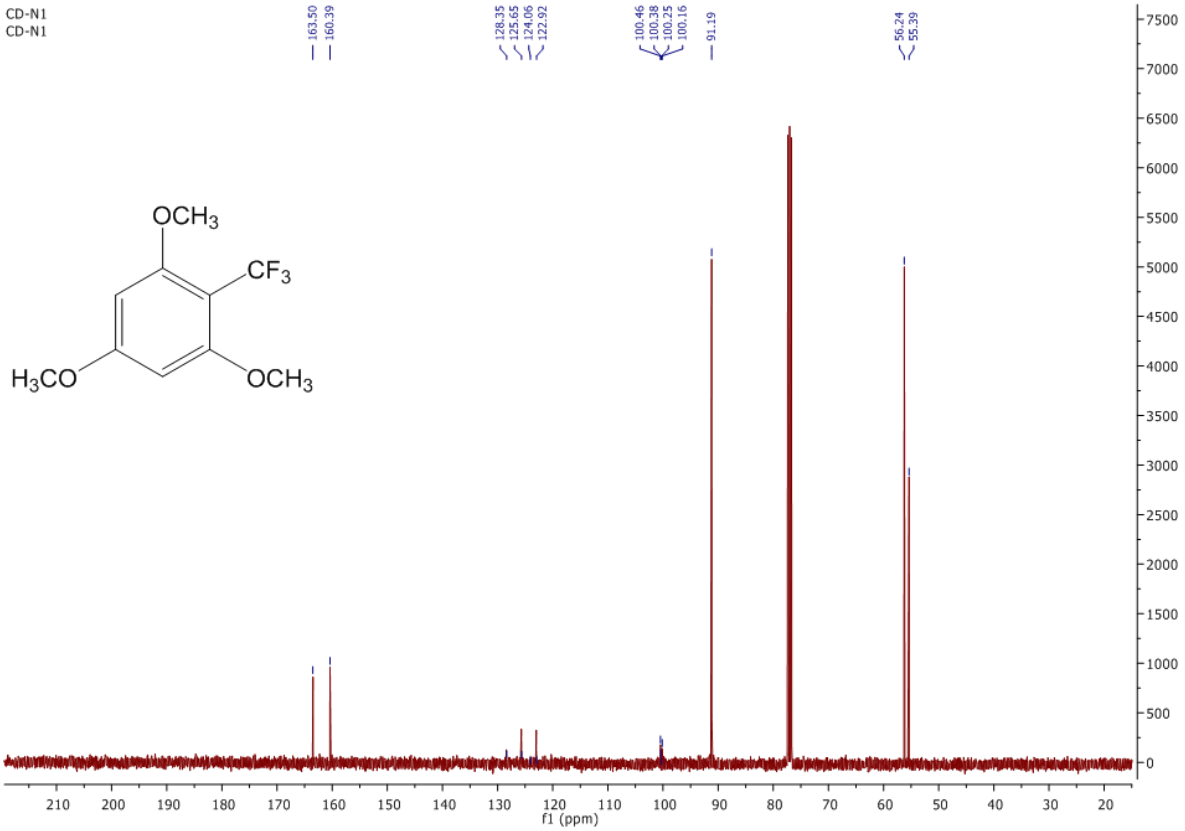

Figure 23: ^{13}C NMR spectra of 1,3,5-trimethoxy-2-(trifluoromethyl)benzene.

Photonic characterization

LED Emission and Reagent Absorbance

The emission spectrum of the used white LED was measured using a setup for diffuse radiometric measurements. The emission of the LED was normalized to the maximum emission. To compare the emission of the used LED with the absorption spectra of the used photoactive species, NBS 500 mM in acetonitrile (Reaction 1) and diacetyl 100 mM in ethyl acetate (Reaction 2) were measured by UV/vis spectroscopy using a Shimadzu UV-1780 benchtop spectrometer and a standard quartz cuvette (d = 1 cm). The NBS solution were measured both directly after preparation (no irrad) and after irradiation for 20 min (irrad 20 min) using the 1×A irradiation module (photon flux = 46 µmol · s^{-1}) utilized for the photoreactions. The absorption spectra of the photoactive species, the emission spectrum of the used white LED and a normalized spectrum of a blacklight CFL are depicted in Figure 25.[4]

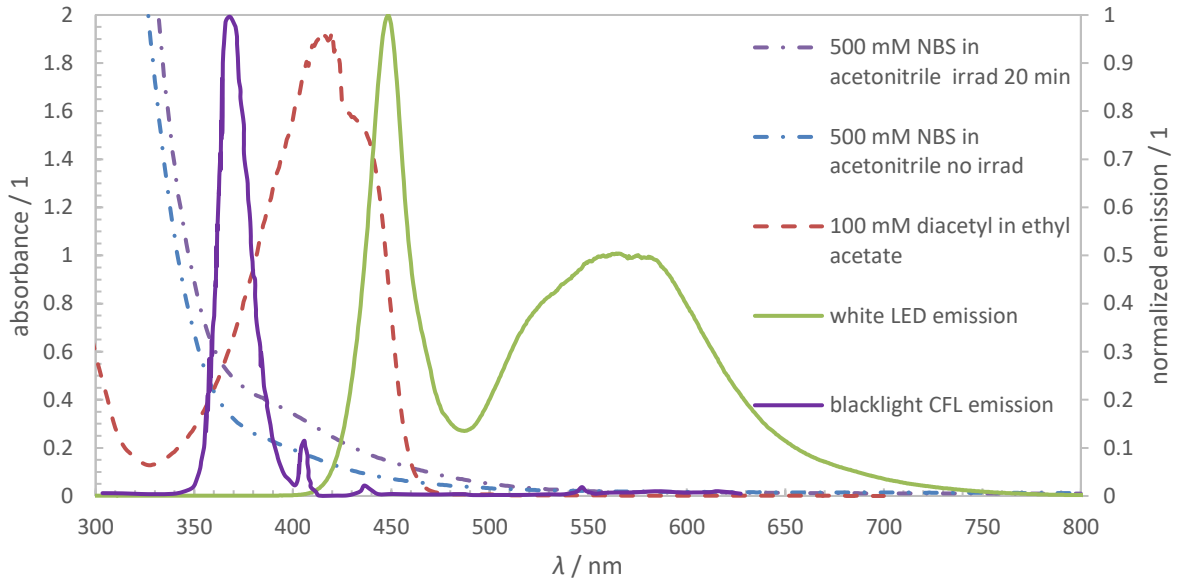

Figure 25: Absorption spectra of NBS 500 Mm in acetonitrile not irradiated (reaction 1) and irradiated for 20 min, diacetyl 100 mM in ethyl acetate (reaction 2) and normalized emission spectra of used white LED and a blacklight CFL.[2]

Comparison of Diffuse and 2D Radiometry

Applying diffuse and 2D radiometric measurements the optical power of the used white LED was determined in dependence of the applied current. The current dependent optical power for both of the used radiometric measurement techniques is depicted in Figure 26.

2D radiometry of the single white LED was performed at a distance of 11.5 cm between the measured light source and the cosine corrector of the spectrometer. The spatially resolved radiometric scans are depicted in Figure 27. Using the optical powers determined by diffuse radiometry as calibration reference, the optical powers of the 2D radiometric scans was corrected by applying the correction factors listed in Table 24.

Table 24: Comparison of optical powers measured for a single white LED using 2D radiometry and diffuse radiometry in dependence of the applied current and resulting experimental correction factors.

2D radiometry		diffuse radiometry		correction factor
Current / mA	**Output / mW**	**Current / mA**	**Output / mW**	
50	194	50	83	0.43
100	421	100	152	0.36
150	607	150	214	0.35
200	789	200	273	0.35
400	1276	400	460	0.36
600	1600	600	587	0.37

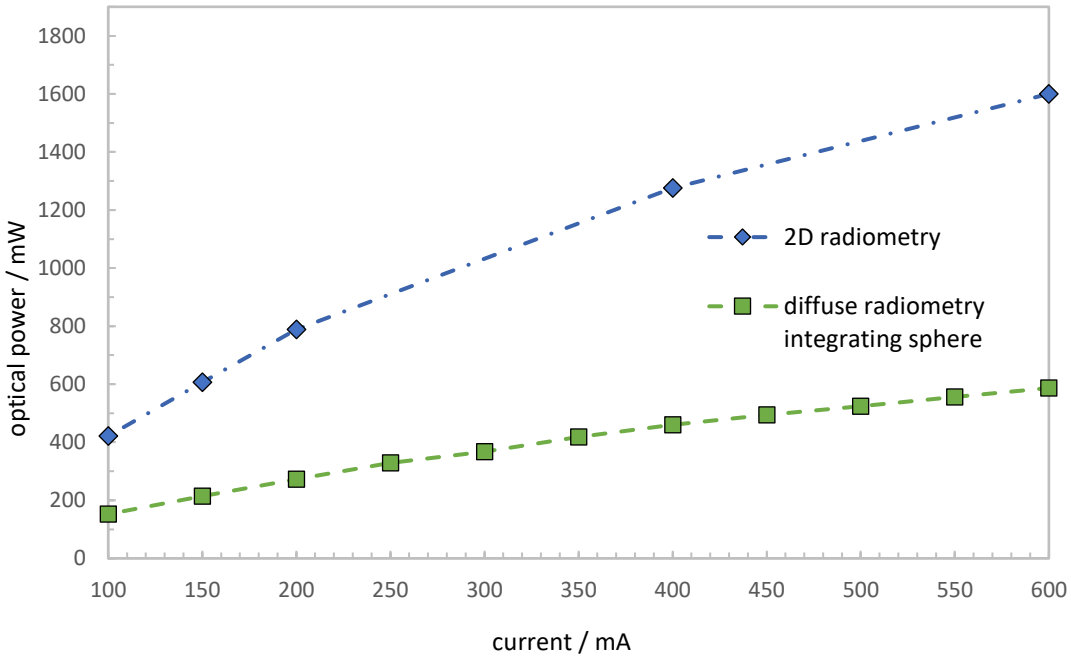

Figure 26: Optical power of a single white LED used for experimentation in dependance of the applied current, measured using calibrated diffuse radiometry and 2D radiometry.

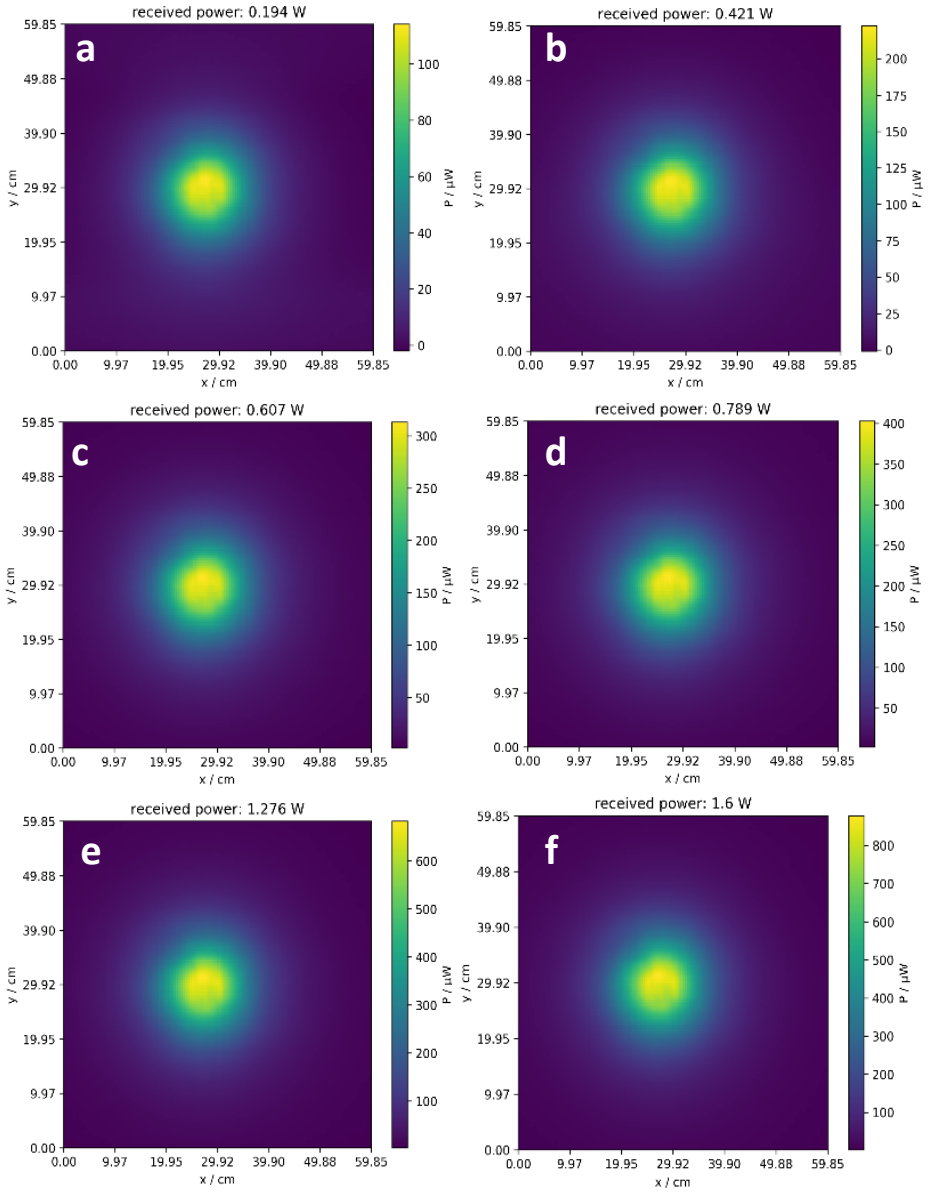

*Figure 27: 2D radiometric scans of a single white LED at **a** 50 mA, **b** 100 mA, **c** 150 mA, **d** 200 mA, **e** 400 A and **f** 600 mA.*

2D radiometry of a 13 white LED array was performed at a distance of 6.5 cm between the measured light source and the cosine corrector of the spectrometer. The spatially resolved radiometric scans are depicted in Figure 28. Using the previously determined calibration factors applied for the 2D radiometric scans of the single white LED on the measurements of the LED arrays, the measured relative optical powers was corrected to the absolute values listed in Table 25.

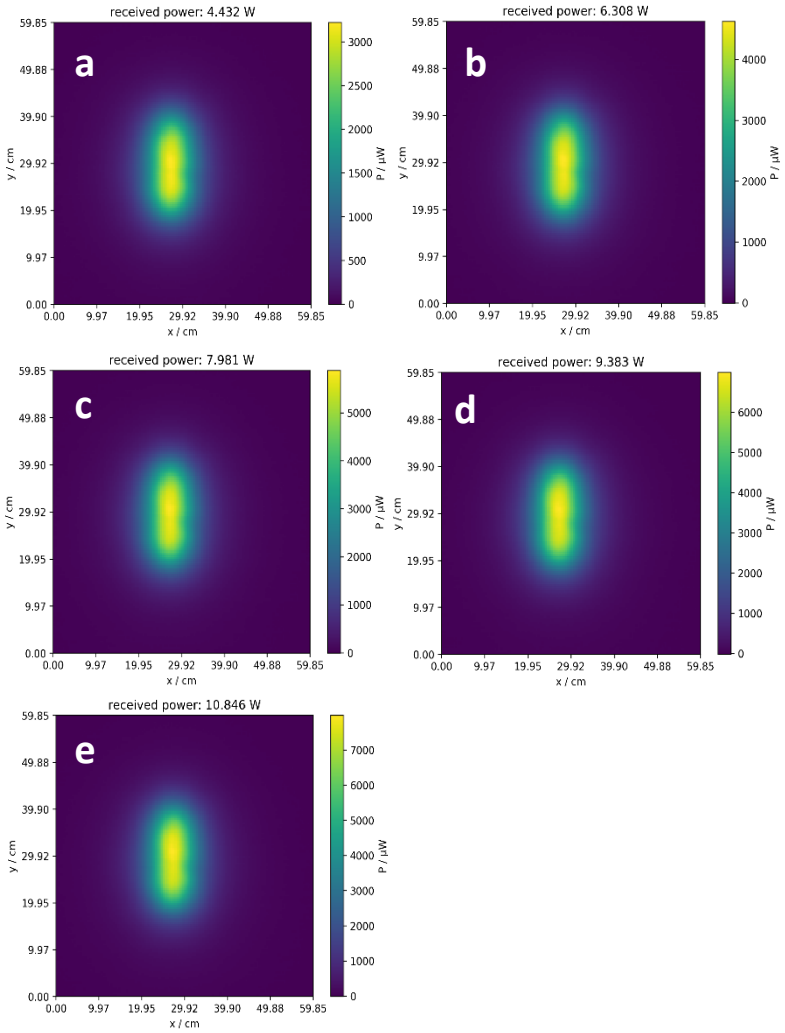

*Figure 28: 2D radiometric scans of an 13 white LED array (LEDs connected in parallel) at **a** 1000 mA, **b** 1500 mA, **c** 2000 mA, **d** 2500 mA and **e** 3000 mA.*

Table 25: Measured and corrected optical powers of an LED array consisting of 13 parallel connected LEDs.

current total / A	amount parallel LEDs	current per LED / mA	optical power measured box / mW	optical power corrected box / mW
1.0	13	76.92	4432	1562
1.5		115.39	6308	2224
2.0		153.85	7981	2813
2.5		192.31	9383	3308
3.0		230.77	10846	3823

Calculation of Angle Dependent Intensity Distribution

The spatially resolved 2D radiometric measurements of a single white LED were used to calculate the opening angle dependent intensity distribution of the light source. Therefore, slices at the maximal intensity of the 2D radiometric scans in x and y direction were determined. The position dependent intensity distribution of the scans of a single white LED and a 13 LED array can be seen in Figure 29. The 2D radiometric scans of the light sources were performed with a distance of 11.5 cm (single LED) and 6.5 cm (13 LED array) between the light source and the cosine corrector of the spectrometer. The corresponding distance is abbreviated as z-position.

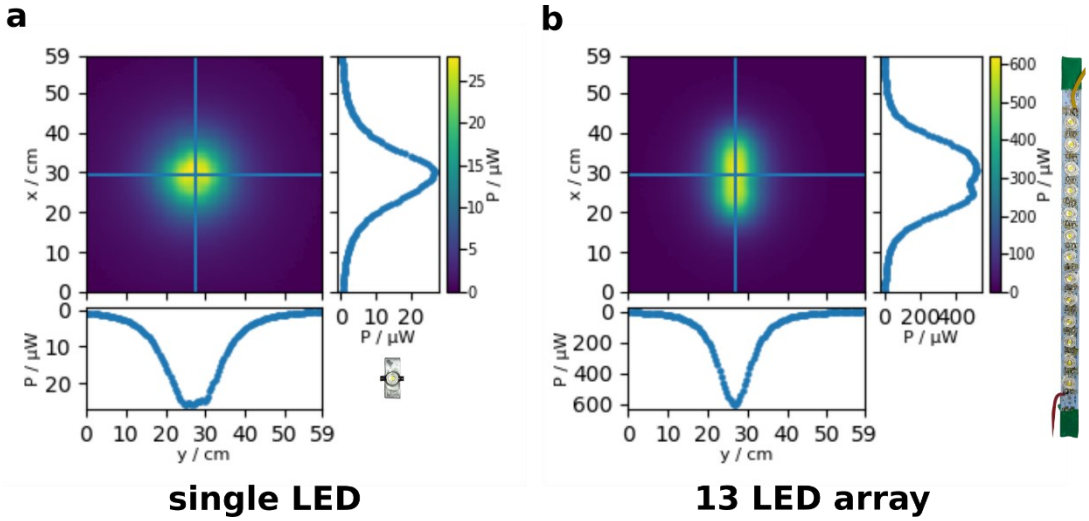

*Figure 29: 2D radiometric scans of a **a** single white LED and an **b** LED array consisting of 13 LEDs.*

The position dependent intensity of a single pixel of a slice in x or y direction can be assigned to an opening angle of the LED using the trigonometric function $arctan(x\ or\ y\ /\ z)$. Normalization of the intensity distribution of the presented x-slice to 1 was performed based on the peak emission of the LED. The resulting angle dependent intensity distribution of a single white LED is depicted in Figure 30.

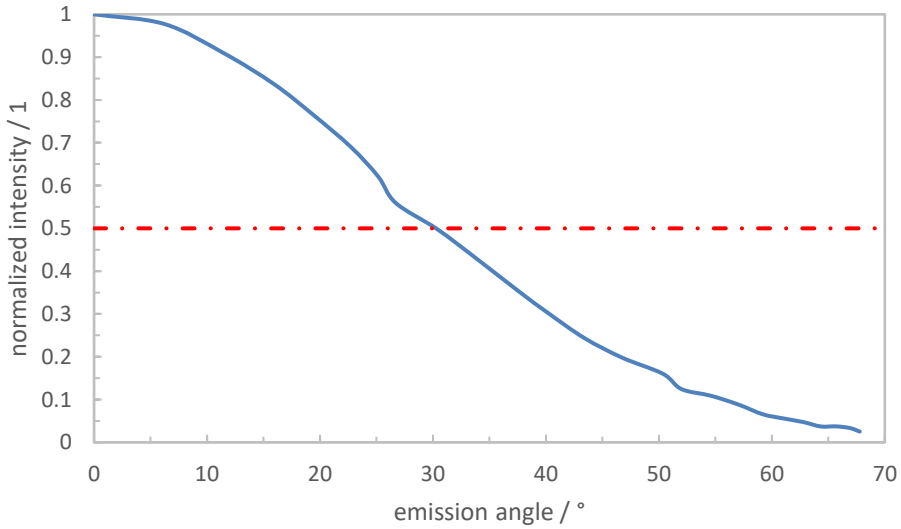

Figure 30: Normalized angle dependent intensity distribution of the used white LED.

Calculation of Wavelength Dependent Transmission

The wavelength dependent transmission was calculated for NBS 500 mM in acetonitrile (reaction 1) based on the absorbance data depicted in Figure 25. The transmission for a film thickness of 206 µm and the diameters of the reservoirs of the corresponding 1×A, 2×A and 4×A reactor modules ($d = 25$ mm, $d = 38$ mm and d = 50 mm) are shown in Figure 31, Figure 32, Figure 33 and Figure 34.

film thickness: 0.206 mm; λ > 400 nm (transmission > 98 %)

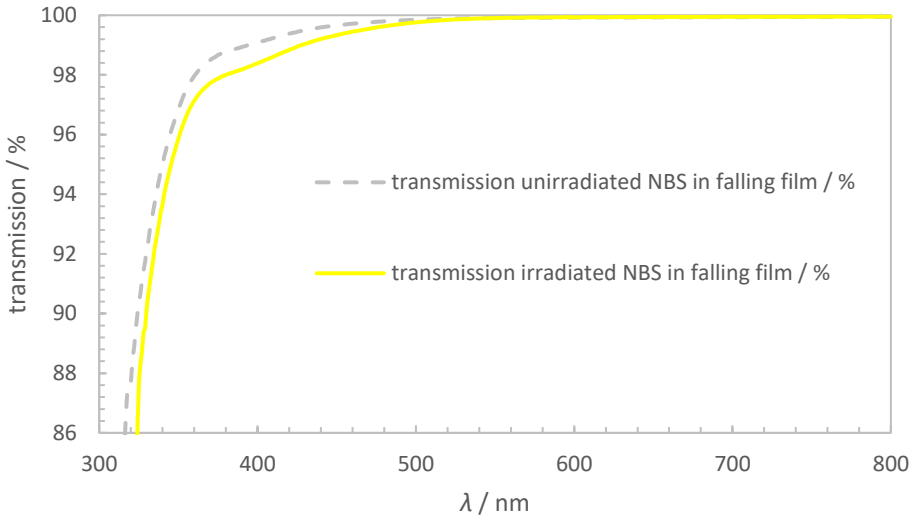

Figure 31: Calculated wavelength dependent transmission of light through a 0.206 mm thick falling film.

diameter reservoir: 25 mm (1×A reactor module)

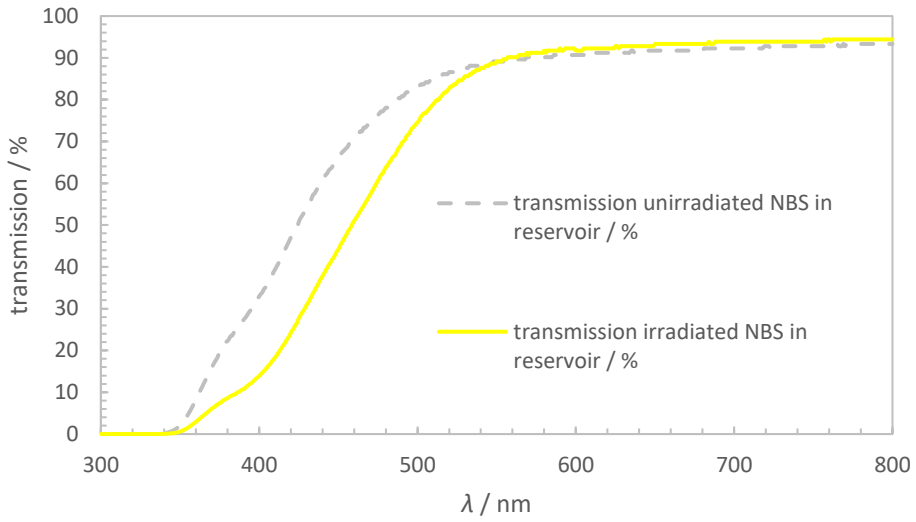

Figure 32: Calculated wavelength dependent transmission of light through the 25 mm diameter reservoir.

diameter reservoir: 38 mm (2×A reactor module)

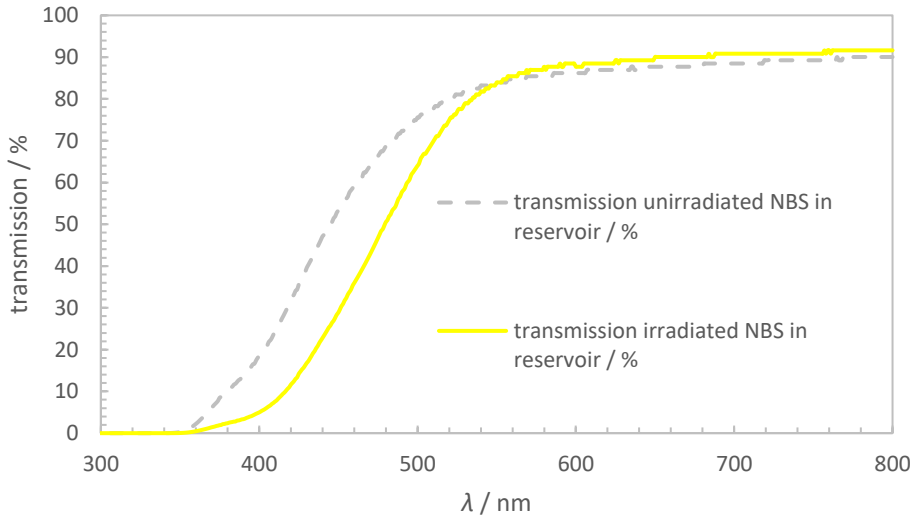

Figure 33: Calculated wavelength dependent transmission of light through the 38 mm diameter reservoir.

diameter reservoir: 50 mm (4×A reactor module)

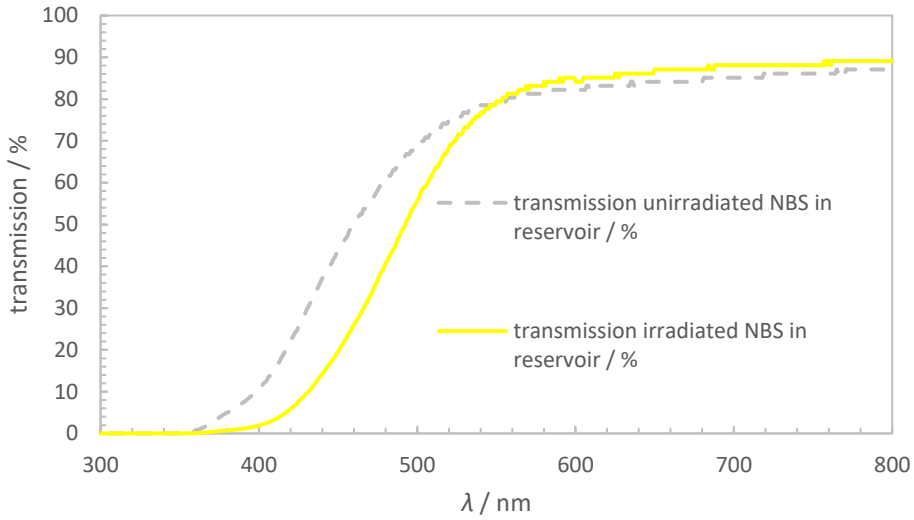

Figure 34: Calculated wavelength dependent transmission of light through the 50 mm diameter reservoir.

Sources

[1] G. Rltzoulls, N. Papadopoulos, D. Jannakoudakls, **1996**, 146–148.

[2] P. K. Chhattise, A. V. Ramaswamy, S. B. Waghmode, *Tetrahedron Lett.* **2008**, *49*, 189–194.

[3] L. Li, X. Mu, W. Liu, Y. Wang, Z. Mi, C. J. Li, *J. Am. Chem. Soc.* **2016**, *138*, 5809–5812.

[4] L. H. Loetscher, J. M. Carey, S. L. Skiles, V. M. Carey, J. E. Boyd, *Ind. Eng. Chem. Res.* **2009**, *48*, 4697–4702.